CHAPTER 17
MICROSCOPES

Shinya Inoué and Rudolf Oldenbourg
Marine Biological Laboratory
Woods Hole, Massachusetts

17.1 GLOSSARY

f	focal length
M	magnification
n	refractive index
NA	numerical aperture
z	distance along optical axis
λ	wavelength of light

17.2 INTRODUCTION

Historic Overview

The optical principles and basic lens design needed to generate a diffraction-limited, highly magnified image with the light microscope were already essentially perfected a century ago. Ernst Abbe demonstrated how a minimum of two successive orders of diffracted light had to be captured in order for a particular spacing to be resolved (see historical sketch about Abbe principle[1]). Thus, he explained and demonstrated with beautiful experiments the role of the wavelength of the imaging light and the numerical aperture (NA, $\mathrm{NA} = n \sin \Theta$, Fig. 1) of the objective and condenser lenses on the resolving power of the microscope. In general, the minimum spacing δ for line gratings that can just be resolved cannot be smaller than

$$\delta = \frac{\lambda}{2\,\mathrm{NA}} \tag{1}$$

when the NA of the condenser is equal to the NA of the objective.

With the NA of the Lister-type objective (Fig. 2*a*) extended by the addition of an aplanatic hyperhemisphere in the Amici-type objective (Fig. 2*b*), and further by the incorporation of homogeneous immersion (Fig. 2*c*), the numerical aperture of the objective lens was raised from around 0.25 to 0.65 and to 1.25. The apochromatic objective (Fig. 2*d*) was introduced in 1986. By incorporating low-dispersion fluorite lens

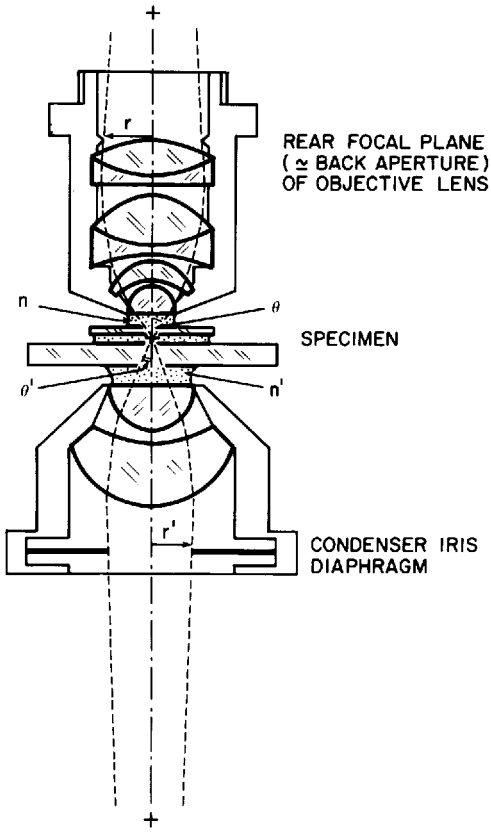

FIGURE 1 Definition of numerical aperture of objective ($NA_{obj} = n \sin \Theta$) and condenser ($NA_{cond} = n' \sin \Theta'$).[6]

elements, the apochromats provided good correction for lateral as well as longitudinal chromatic aberration up to an NA of 1.35 when used in conjunction with a compensating eyepiece, albeit with residual error of the secondary spectrum and appreciable curvature of field. Early high-resolution compound microscopes were equipped with an (oil-immersible) Abbe condenser whose iris diaphragm, placed at the front focal plane of the condenser, could be off-centered to achieve oblique illumination.

Much of the early use of the light microscope depended on the relatively high image contrast that could be generated by differential absorption, reflection, birefringence, etc., due to specimen composition or structure. Specimens, such as unstained living cells and other transparent objects introducing small optical path differences, were generally not amenable to direct microscopic observation for they would not produce detectable image contrast when brought to exact focus.

These impediments were removed by Zernicke who showed how contrast in the microscope image is generated by interference between the light waves that make up the direct rays (that are undeviated by the specimen) and those that were scattered and suffered a phase difference by the presence of the specimen. Using this principle, Zernicke invented the phase contrast microscope.[2] For the first time it became possible to see, in focus, the image of small, nonabsorbing objects. Zernicke's revelations, together with

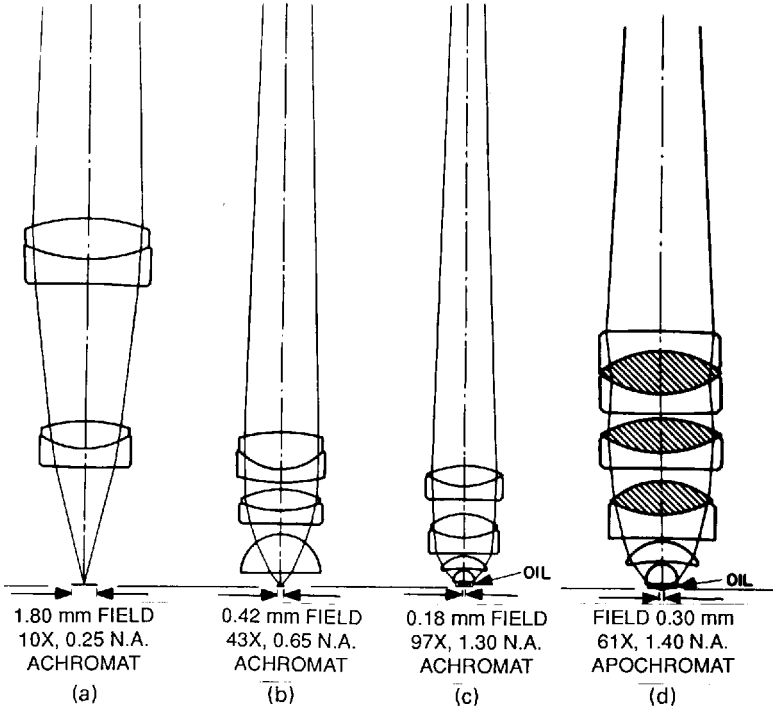

FIGURE 2 (*a*) Lister-type, (*b*) Amici-type, and (*c*) oil-contacted achromatic objectives. In (*d*) an apochromat is shown, with fluorite elements shaded.[57]

Gabor's further contributions,[3] not only opened up opportunities for the design of various types of interference-dependent image-forming devices but, even more importantly, improved our understanding of the basic wave optics involved in microscope image formation.

About the same time as Zernicke's contributions, perfection of the electron microscope made it possible to image objects down to the nanometer range, albeit necessitating use of a high-vacuum environment and other conditions compatible with electron imaging. Thus, for four decades following World War II, the light microscope in many fields took a back seat to the electron microscope.

During the last decade, however, the light microscope has reemerged as an indispensable, powerful tool for investigating the submicron world in many fields of application. In biology and medicine, appropriate tags, such as fluorescent and especially immunofluorescent tags, are used to signal the presence and location of selected molecular species with exceptionally high sensitivity. Dynamic behavior of objects far below the limit of resolution are visualized by digitally-enhanced video microscopy directly in their natural (e.g., aqueous) environment. Very thin optical sections are imaged by video microscopy, and even more effectively with confocal optics. Quantitative measurements are made rapidly with the aid of digital image analysis.

At the same time, computer chips and related information-processing and storage devices, whose availability in part has spurred the new developments in light microscopy, are themselves miniaturized to microscopic dimensions and packaged with increasingly higher density. These electronic and photonic devices in turn call for improved means for mass manufacturing and inspection, both of which require advanced microscope optics.

Driven by the new needs and aided in part by computerized ray tracing and the introduction of new optical materials, we see today another epochal advance in the quality of lens design. The precision and remote control capabilities of mechanical components are also steadily improving. Furthermore, we may expect another surge of progress, hand-in-hand with development of improved electro-optical and electromechanical devices, in regulated image filtration, contrast-generating schemes, as well as in optical manipulation of the specimen employing microscope optics.

Outline

In the following, we first review the general optical considerations that enter into the use and design of the light microscope, examine several commonly used modes of contrast generation, discuss additional modes of microscopy, list some applications in which the microscope is used to optically manipulate the specimen, and describe some accepted mechanical standards.

Many of the above subjects which are introduced here in the context of microscopy are discussed in more detail in other chapters of this Handbook. On general optical considerations consult Handbook chapters on Geometric Optics (Vol. I, Chap. 1) and on Optical Elements, such as Lenses (Vol. II, Chap. 1), Mirrors (Vol. II, Chap. 2), Polarizers (Vol. II, Chap. 3), etc., as well as chapters on Physical Optics for wave phenomena such as Interference (Vol. I, Chap. 2), Diffraction (Vol. I, Chap. 3), Coherence (Vol. 1, Chap. 4), and Polarization (Vol. I, Chap. 5) which, as phenomena, are essential to the workings of the various contrast modes of the microscope. Material on image detection and processing can be found in Handbook articles on Vision, Imaging Detectors, and Optical Information and Image Processing.

There are a number of excellent review articles and books discussing the optical principles of light microscopes[1,4,5] and microscopic techniques[6–8] and their applications.[9–11] The present article is intended in part to bridge the territories of the manufacturer and the user of the microscope, including those who incorporate microscope optics into other equipment or apply them in unconventional ways. Thus, the article emphasizes basic principles and does not attempt to discuss specialized instruments such as operating microscopes, specific inspection microscopes, etc.

17.3 GENERAL OPTICAL CONSIDERATIONS

Geometrical and Wave Optical Train, Magnification

In an optical train of a conventional microscope (Fig. 3), the objective lens L_{ob} projects an inverted, real, magnified image O' of the specimen O (or object) into the intermediate

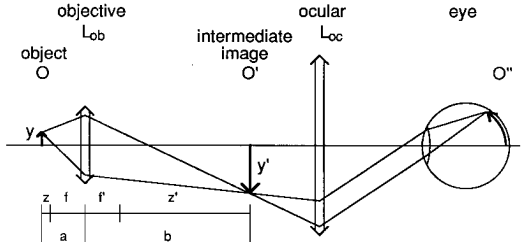

FIGURE 3 Ray path in the microscope from object to observer's eye (see text).

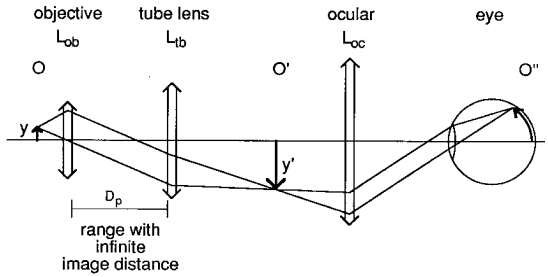

FIGURE 4 Ray path in microscope with infinity-corrected objective and tube lens.

image plane (or primary image plane). The intermediate image plane is located at a fixed distance $f' + z'$ behind L_{ob}, where f' is the back focal length of L_{ob} and z' is the optical tube length of the microscope. In general, O' is an aerial image for which an ocular L_{oc} (or the eyepiece) acts as a magnifier in front of the eye. Since L_{oc}, coupled with the corneal surface and lens of the eye, produces an erect image O'' of O on the retina, the object appears inverted to the observer. The ocular may conversely be used as a projector.

Continuing with the schematic diagram in Fig. 3, using thin-lens approximations, O is placed at a short distance z just outside of the front focus of L_{ob}, such that $z + f = a$, where f is the front focal length of L_{ob} and a is the distance between O and L_{ob}. O' is formed at a distance $b = (z' + f')$ behind L_{ob}. For a height y of O, the image height $y' = y \times b/a$. Thus, L_{ob} magnifies O by $M_{ob} = b/a$. Also, $M_{ob} = f/z = z'/f'$. M_{ob} is the transverse magnification (or lateral magnification) of L_{ob}. In turn, y' is magnified by L_{oc} by a factor $M_{oc} = 25\text{ cm}/f_{oc}$, where f_{oc} is the focal length of the ocular and 25 cm is the so-called near distance from the observer's eye (see section on Vision in this Handbook). Thus, the total transverse magnification of the microscope $M_{tot} = M_{ob} \times M_{oc}$.

Note that most microscope objectives are corrected for use only within a narrow range of image distances, and, in general, only in conjunction with specific groups of oculars. M_{ob}, which is the magnification inscribed on the barrel of the objective lens, is defined for its specified tube length (for high-power objectives, $M_{ob} = z'/f$). In the case of an infinity-corrected objective, M_{ob} is the ratio y'/y as used in conjunction with a specific tube lens L_{tb} (Fig. 4). These factors, as well as those mentioned under "Microscope Lenses, Aberrations," must be kept in mind when a microscope objective is used as a magnifying lens, or in reverse as a high-numerical-aperture reducing lens, to form a truly diffraction-limited image.

Conjugate Planes

Continuing the optical train back to the light source in a transilluminating microscope, Fig. 5*a* shows the ray paths and foci of the waves that focus on an on-axis point in the specimen. In Köhler illumination, the distance between the specimen and the condenser are adjusted so that the image of the field diaphragm in the illuminator is superimposed with the focused region of the specimen, and the lamp collector lens is adjusted so that the source image is focused in the plane of the condenser aperture diaphragm. Thus, $\bar{O}$, O, O', and O'' all lie in image planes that are conjugate with each other.

Tracing the rays emitted from a point in the light source (Fig. 5*b*), the rays are parallel between the condenser and the objective lenses, thus the specimen is illuminated by a plane wavefront. This situation arises because the iris diaphragm of the condenser is built into the front focal plane of the condenser. Also, since the pupil of an (experienced)

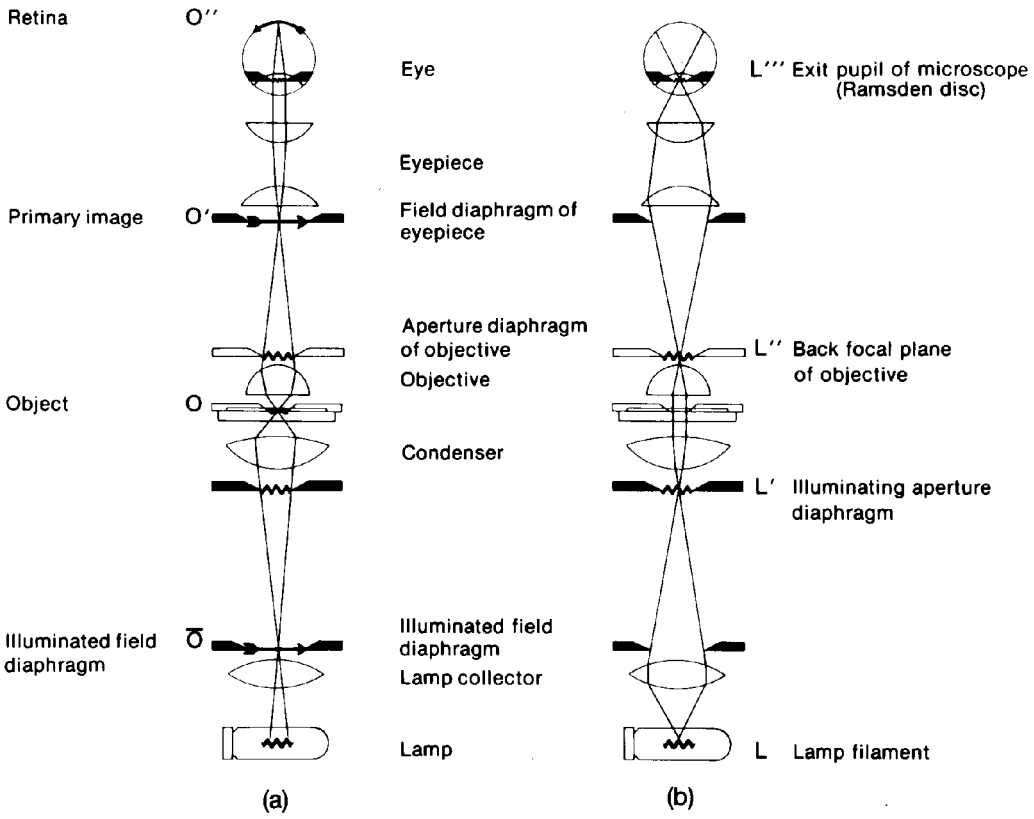

FIGURE 5 Ray paths in a transmitted light microscope adjusted for Köhler illumination. Two sets of conjugate planes are shown: set O in (a) is conjugate with the object O and with the field diaphragm planes; set L in (b) is conjugate with the lamp filament L and with aperture diaphragm planes.[58]

observer's eye is placed at the eyepoint or back focal plane of the ocular, the four aperture planes L, L', L'', and L''' are again conjugate to each other.

As inspection of these two figures shows, the field planes and aperture planes are in reciprocal space relative to each other throughout the whole optical system. This reciprocal relationship explains how the various diaphragms and stops affect the cone angles, paths, and obliquity of the illuminating and image-forming rays, and the brightness, uniformity, and size of the microscope field. More fundamentally, a thorough grasp of these reciprocal relationships is needed to understand the wave optics of microscope image formation and for designing various contrast-generating devices and other microscope optical systems.

Airy Disk and Lateral Resolution

Given a perfect objective lens and an infinitely small point of light residing in the specimen plane, the image formed in the intermediate image plane by the objective lens is not another infinitely small point, but a diffraction image with a finite spread (Fig. 6*a*). This Airy diffraction image is the Fraunhofer diffraction pattern formed by the exit pupil of the

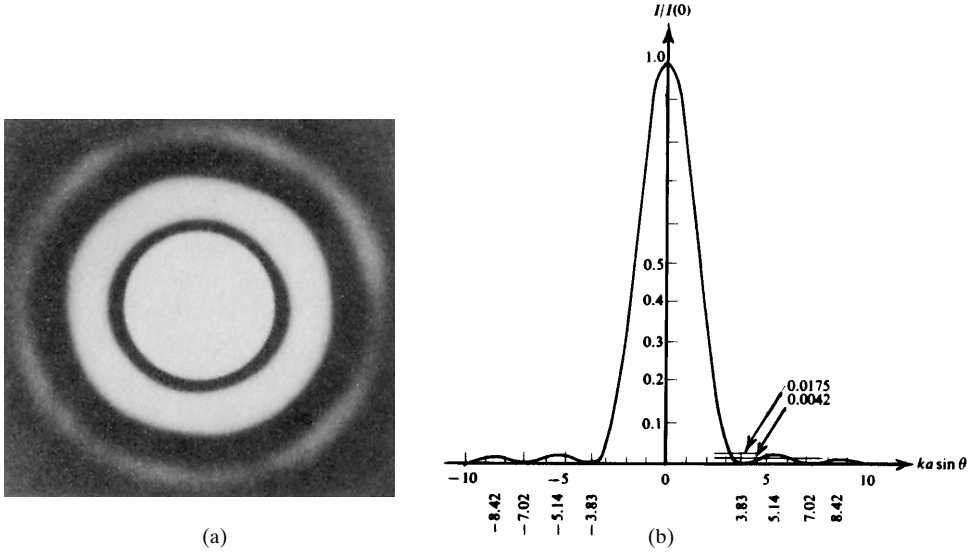

FIGURE 6 Airy pattern of circular aperture: image (*a*) of central Airy disk, first dark ring and subsidiary maximum; graph (*b*) of radial intensity distribution.[59]

objective lens from which spherical waves converge to the focal point. The distribution of irradiance of the diffraction image (Fig. 6*b*) is given by an expression containing the first order Bessel function $J_1(v)$:

$$I(v) = I_0\left(\frac{2J_1(v)}{v}\right)^2 \tag{2}$$

with v proportional to the diffraction angle. If the irradiance is calculated as a function of radius measured from the center of the Airy diffraction pattern located in the intermediate image plane, v takes on the form:

$$v = 2\pi\frac{\mathrm{NA}}{M\lambda}r_i \tag{3}$$

where NA is the numerical aperture and M the magnification of the objective lens, λ the wavelength of light, and r_i the radial distances measured in the intermediate image plane. If we express r_i as a distance r_o in object space, with $r_i = Mr_o$, we obtain the more familiar relationship:

$$v = 2\pi\frac{\mathrm{NA}}{\lambda}r_o \tag{4}$$

The central bright disk of the diffraction image is known as the Airy disk, and its radius (the radius from the central peak to the first minimum of the diffraction image) in object space units is given by:

$$r_{\mathrm{Airy}} = 0.61\frac{\lambda}{\mathrm{NA}} \tag{5}$$

When there exist two equally bright, self-luminous points of light separated by a small distance d in object space, i.e., the specimen plane, their diffraction images lie side-by-side

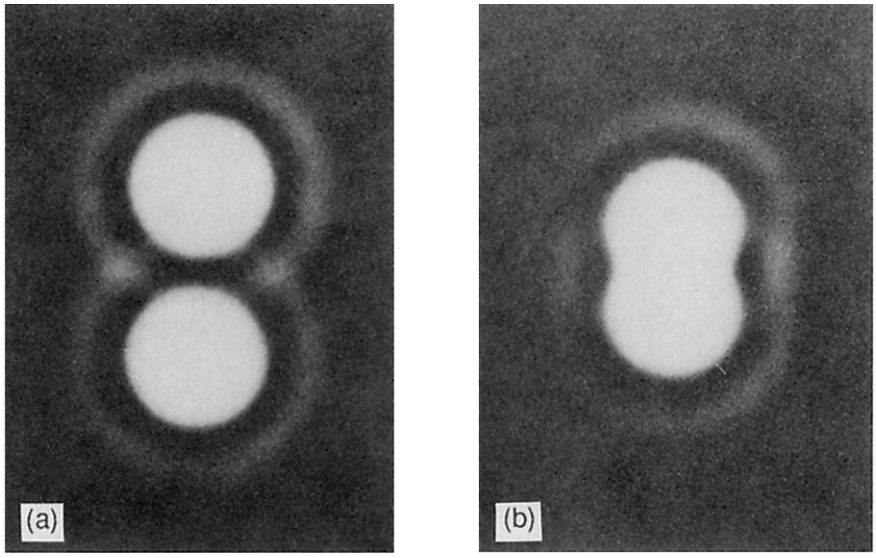

FIGURE 7 Overlapping Airy patterns: (*a*) clearly resolved; (*b*) center of Airy patterns separated by $d = r_{\text{Airy}}$, Rayleigh criterion.[59]

in the image plane. The sum of the two diffraction images, assuming the two points of light were mutually incoherent, appears as in Fig. 7*a*. As d becomes smaller so that the first minimum of one diffraction image overlaps with the central maximum of the neighboring diffraction image ($d = r_{\text{Airy}}$, Fig. 7*b*), their sum (measured along the axis joining the two maxima) still contains a dip of 26.5 percent of the peak intensities that signals the twoness of the source points (the Rayleigh criterion). Once d becomes less than this distance, the two diffraction images rapidly pass a stage where instead of a small dip, their sum shows a flat peak (the Sparrow criterion) at $d = 0.78\ r_{\text{Airy}}$, and thereafter the sum of the diffraction images appears essentially indistinguishable from one arising from a single point source instead of two. In other words, we can no longer resolve the image of the two points once they are closer than the Rayleigh criterion, and we lose all cues of the periodicity at spacings below the Sparrow criterion. Since the diameter of the Airy diffraction image is governed by NA_{obj} and the wavelength of the image-forming light λ, this resolution limit normally cannot be exceeded (for exceptions, see the sections on ''Confocal Microscopy'' and ''Proximity Scanning Microscopy'' later in this chapter).

The consideration given here for two point sources of light applies equally well to two absorbing dots, assuming that they were illuminated incoherently. (Note, however, that it may, in fact, be difficult or impossible to illuminate the two dots totally incoherently since their spacing may approach the diameter of the diffraction image of the illuminating wave. For the influence of the condenser NA on resolution in transillumination, refer to the section on ''Transillumination'' later in this chapter. Also, the contrast of the diffraction images of the individual absorbing dots diminishes rapidly as their diameters are decreased, since the geometrical size of such small dots would occupy a decreasing fraction of the diameter of their diffraction images. For further detail see Ref. 12.)

The image of an infinitely small point or line thus acquires a diameter equal to that of the Airy disk when the total magnification of the image becomes sufficiently large so that we can actually perceive the diameter of the Airy disk. In classical microscopy, such a large magnification was deemed useless and defined as empty magnification. The situation is, however, quite different when one is visualizing objects smaller than the limit of resolution

with video microscopy. The location of the Airy disk can, in fact, be established with very high precision. Distances between lines that are clearly isolated from each other can, therefore be measured to a precision much greater than the resolution limit of the microscope. Also, minute movements of nanometer or even Ångstrom steps have been measured with video-enhanced light microscopy using the center of gravity of the highly magnified diffraction image of marker particles.[13]

Three-dimensional Diffraction Pattern, Axial Resolution, Depth of Focus, Depth of Field

The two-dimensional Airy pattern that is formed in the image plane of a point object is, in fact, a cross section of a three-dimensional pattern that extends along the optical axis of the microscope. As one focuses an objective lens for short distances above and below exact focus, the brightness of the central spot periodically oscillates between bright and dark as its absolute intensity also diminishes. Simultaneously, the diameters of the outer rings expand, both events taking place symmetrically above and below the plane of focus in an aberration-free system (Fig. 8).

Figure 9*c* shows an isophot of the longitudinal section of this three-dimensional diffraction image. In the graph we recognize at $v = 1.22\pi$ (and $u = 0$, focal plane) the first minimum of the Airy pattern which we discussed in the previous section. The intensity distribution along u perpendicular to the focal plane has its first minima at $u = \pm 4\pi$ and $v = 0$ ($\pm z_1$ in Fig. 9*a*).

To find the actual extent of the three-dimensional diffraction pattern near the intermediate plane of the microscope, we express the dimensionless variables v and u of Fig. 9*c* as actual distances in image space. The relationship between v and the lateral distance r_i is given by Eq. (3). The axial distance z_i, oriented perpendicular to the image plane, is related to u by:

$$u = 2\pi \frac{\mathrm{NA}^2}{M^2 \lambda} z_i \tag{6}$$

The first minimum ($u = 4\pi$) is at a distance $z_1 = (2M^2\lambda)/\mathrm{NA}^2$. To transfer distance z_i in image space to distance z_o in object space, we use the relationship $z_i = z_o M^2/n$. (Note that for small axial distances, to a close approximation, the axial magnification is the square of the lateral magnification M divided by the refractive index n of the object medium.) The distance from the center of the three-dimensional diffraction pattern to the first axial minimum in object space is then given by:

$$z_{\min} = 2 \frac{\lambda n}{\mathrm{NA}^2} \tag{7}$$

$z_{\min}$ corresponds to the distance by which we have to raise the microscope objective in order to change from exact focus of a small pinhole to the first intensity minimum in the center of the observed diffraction pattern (see Fig. 8).

In correspondence to the lateral resolution limit which is taken as the Airy disk radius r_{Airy} [Eq. (5)], we can use $z_{\min}$ as a measure of the limit of axial resolution of microscope optics. Note that the ratio of axial to lateral resolution ($z_{\min}/r_{\mathrm{Airy}} = 3.28\, n/\mathrm{NA}$) is inversely proportional to the numerical aperture of the objective.

The axial resolution of the microscope is closely related to the depth of focus, which is the axial depth on both sides of the *image* plane within which the image remains acceptably sharp (e.g., when a focusing screen at the image plane is displaced axially without moving the object or objective). The depth of focus D is usually defined as $\frac{1}{4}$ of the axial distance between the first minima above and below focus of the diffraction image of a small pinhole. In the intermediate image plane, this distance is equal to $z_1/2$, with z_1 defined earlier. The depth of focus defined by z_1 is the diffraction-limited, or physical, depth of focus.

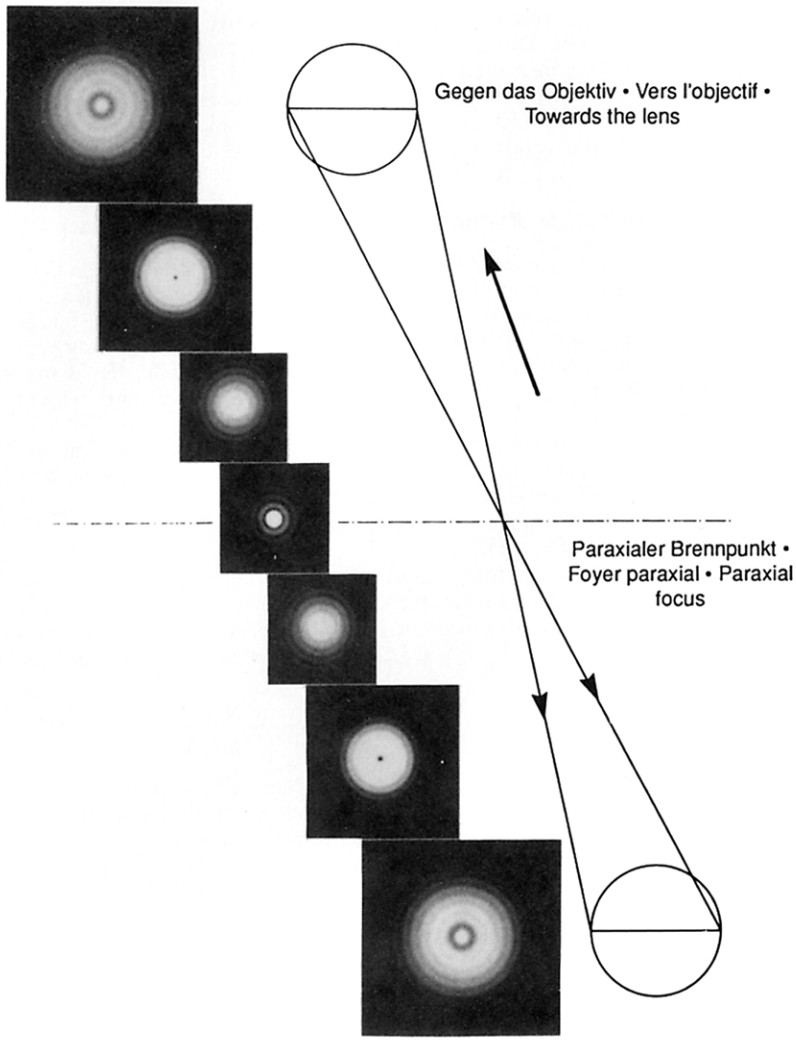

FIGURE 8 The evolution of the diffraction image of a circular aperture with differing planes of focus in an aberration-free system.[60]

A second and sometimes dominating contribution to the total depth of focus derives from the lateral resolution of the detector used to capture the image. This geometric depth of focus depends on the detector resolution and the geometric shape of the light cone converging to the image point. If the detector is placed in the intermediate image plane of an objective with magnification M and numerical aperture NA, the geometrical depth of focus D is given by

$$D = \frac{M}{\mathrm{NA}} e \tag{8}$$

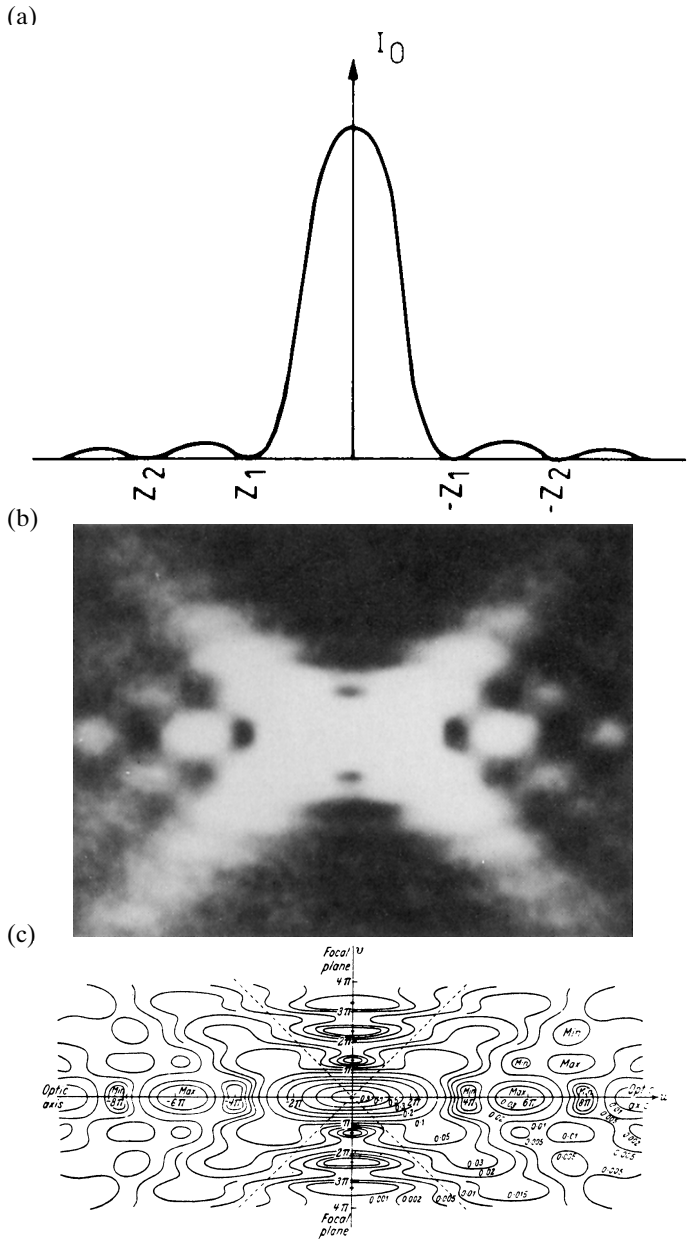

FIGURE 9 (*a*) Axial intensity distribution of irradiance near focal point;[15] (*b*) meridional section through diffraction pattern near focal point of a point source of light focused by lens with a uniform circular aperture;[15] (*c*) contour plot (isophot) of the same cross section as in (*b*).[35] The three-dimensional diffraction pattern is obtained by rotating the meridional section around the optic axis. The three-dimensional diffraction pattern is also called the intensity point spread function.

with e the smallest distance resolved by the detector (e is measured on the detector's face plate).

The depth in *specimen* space that appears to be in focus within the image, without readjustment of the microscope focus, is the depth of field (unfortunately often also called the depth of focus). To derive expressions for the depth of field, we can apply the same arguments as outlined above for the depth of focus. Instead of moving the image plane in and out of focus, we keep the image plane in the ideal focus position and move the small pinhole in object space. Axial distances in object space, however, are a factor n/M^2 smaller than corresponding distances in image space. Therefore, we apply this factor to the expression for the geometrical depth of focus [Eq. (8)] and add the physical depth of field [derived from Eq. (7)] for the total depth of field d_{tot}:

$$d_{\text{tot}} = \frac{\lambda n}{\text{NA}^2} + \frac{n}{M\text{NA}} e \tag{9}$$

Notice that the diffraction-limited depth of field shrinks inversely proportionally with the square of the NA, while the lateral limit of resolution is reduced inversely proportionally to the first power of the NA. Thus, the axial resolution and thinness of optical sections that can be attained are affected by the system NA much more so than is the lateral resolution of the microscope.

These values for the depth of field, and the distribution of intensities in the three-dimensional diffraction pattern, are calculated for incoherently illuminated (or emitting) point sources (i.e., $\text{NA}_{\text{cond}} \geq \text{NA}_{\text{obj}}$). In general, the depth of field increases, up to a factor of two, as the coherence of illumination increases (i.e., as $\text{NA}_{\text{cond}} \to 0$). However, the three-dimensional point spread function with partially coherent illumination can depart in complex ways from that so far discussed when the aperture function is not uniform (see sections on ''Phase Contrast and Other Aperture-modifying Contrast Modes,'' ''Polarizing,'' and ''Interference'' later in this chapter). In a number of phase-based, contrast-generating modes of microscopy, the depth of field may turn out to be unexpectedly shallower than that predicted from Eq. (9) and may yield extremely thin optical sections.[14]

17.4 MICROSCOPE LENSES, ABERRATIONS

Designations of Objective Lenses

With few exceptions, microscope objective lenses are designed to form a diffraction-limited image in a specific image plane that is located at a fixed distance from the objective lens (or from the tube lens in the case of an infinity-focus system). The field of view is often quite limited, and the front element of the objective is placed close to the specimen with which it must lie in optical contact through a medium of defined refractive index (see Sects. ''Coverslip Correction,'' ''Tube Lengths and Tube Lenses for which Microscope Objectives Are Corrected,'' and ''Mechanical Standards'' later in this chapter) for standardized distances commonly used for microscope objectives).

Depending on the degree of correction, objectives are generally classified into achromats, fluorites, and apochromats with a plan designation added to lenses with low curvature of field and distortion (Table 1). Some of these characteristics are inscribed on the objective lens barrel, such as Plan Apo 60/1.40 oil 160/0.17, meaning 60 power/1.40 NA Plan Apochromatic objective lens designed to be used with oil immersion between the objective front element and the specimen, covered by an 0.17-mm-thick coverslip, and used at a 160-mm mechanical tube length. Another example might be Epiplan-Neofluar

TABLE 1 Objective Lens Types and Corrections

Type	Spherical	Chromatic	Flatness
Achromat	*	2λ	No
F-Achromat	*	2λ	Improved
Neofluar	3λ	<3λ	No
Plan-Neofluar	3λ	<3λ	Yes
Plan Apochromat	4λ	>4λ	Yes

* = corrected for two wavelengths at two specific aperture angles.
2λ = corrected for blue and red (broad range of visible spectrum).
3λ = corrected for blue, green, and red (full range of visible spectrum).
4λ = corrected for dark blue, blue, green, and red.
***Source*:** Zeiss publication #41-9048/83.

50×/0.85 ∞/0, which translates to Plan ''Fluorite'' objective designed for epi-illumination (i.e., surface illumination of specimen through the objective lens rather than through a separate condenser) with a 50× magnification and 0.85 NA to be used in air (i.e., without added immersion medium between the objective front element and coverslip or specimen), with no coverslip, and an (optical) tube length of infinity. ''Infinity corrected'' objectives may require the use of a designated tube lens to eliminate residual aberration and to bring the rays to focus into the image plane. Achromats are usually not designated as such, and several other codes are inscribed or color-coded on microscope objectives (Tables 2 and 3).

Most objective lenses are designed to be used with a specified group of oculars or tube lenses that are placed at specific distances in order to remove residual errors. For example, compensation oculars are used in conjunction with apochromatic and other high-NA objectives to eliminate lateral chromatic aberration and improve flatness of field. However, some lenses such as Nikon CF (Chrome Free) and current Zeiss Jena objectives are fully corrected so as not to require additional chromatic correction by a tube lens or the ocular.

Coverslip Correction

For objective lenses with large NAs, the optical properties and thicknesses of the media lying between its front element and the specimen critically affect the calculations needed to satisfy the aplanatic and sine conditions and otherwise to correct for image aberrations. For homogeneous immersion objectives (that are designed to be used with the refractive indices and dispersion of the immersion oil, coverslip, and medium imbibing the specimen, all matched to that of the objective lens front element), the calculation is straightforward since all the media can be considered an extension of the front lens element.

However, with nonimmersion objectives, the cover glass can become a source of chromatic aberration which is worse the larger the dispersion and the greater the thickness of the cover glass. The spherical aberration is also proportional to the thickness of the cover glass. In designing objectives not to be used with homogeneous immersion, one assumes the presence of a standard cover glass and other specific optical media between the front lens element and the specimen. As one departs from these designated conditions, spherical aberration (and also coma) increases with the NA of the lens, since the difference between the tangent and sine of the angle of incidence is responsible for departure from the needed sine condition.

It should also be noted that oil immersion objectives fail to provide full correction, or full NA, when the specimen is mounted in an imbibing medium with a different refractive index, e.g., aqueous media, even with the objective and cover glass properly oil-contacted to each other. With such an arrangement, the diffraction image can degrade noticeably as one focuses into the specimen by as little as a few micrometers.[15] Special water immersion

TABLE 2 Common Abbreviations Designating Objective Lens Types

DIC, NIC	Differential (Nomarski) interference contrast
L, LL, LD, LWD, ELWD, ULWD	Long working distance (extra-) (ultra-)
FL, FLUOR, NEOFLUOR, FLUOTAR	With corrections as with "fluorite" objectives but no longer implies the inclusion of fluorite elements
PHASE, PHACO, PC, PH 1, 2, 3, etc.	Phase contrast, using phase condenser annulus 1, 2, 3, etc.
DL, DM, PLL, PL, PM, PH, NL, NM, NH	Phase contrast: dark low, dark medium, positive low low, low, medium, high contrast (regions with higher refractive index appear darker); negative low, medium, high contrast (regions with higher refractive index appear lighter)
PL, PLAN; EF	Flat field; extended field (larger field of view but not as high as with PLAN, achromats unless otherwise desginated)
PLAN APO	Flat field apochromat
NPL	Normal field of view plan
P, PO, POL	Low birefringence, for polarized light
UV	UV transmitting (down to approx. 340 nm), for UV-excited epifluorescence
ULTRAFLUAR	Fluorite objective for imaging down to approx. 250 nm in UV as well as in the visible range
CORR, W/CORR	With correction collar
I, IRIS, W/IRIS	Adjustable NA, with iris diaphragm built into back focal plane
M	Metallographic
NC, NCG	No coverslip
EPI	Surface illumination (specimen illuminated through objective lens), as contrasted to dia- or transillumination
BD, HD	For use in bright or darkfield (hell, dunkel)
CF	Chrome-free (Nikon: objective independently corrected longitudinal chromatic aberrations at specified tube length)
ICS	Infinity color-corrected system (Carl Zeiss: objective lens designed for infinity focus with lateral and longitudinal chromatic aberrations corrected in conjunction with a specified tube lens)
OIL, HI, H; WATER, W; GLY	Oil-immersion, Homogeneous-immersion, water-immersion, glycerol-immersion
U, UT	Designed to be used with universal stage (magnification/NA applies for use with glass hemisphere; divide both values by 1.51 when hemisphere is not used)
DI; MI; TI Michelson	Interferometry: noncontact; multiple-beam (Tollanski);
ICT; ICR	Interference contrast: in transillumination; in reflected light

objectives (e.g., Nikon Plan Apo 60×/1.2 NA and short-wavelength transmitting Fluor 40×/1.0 NA, both with collar to correct coverslip thickness deviation from 0.17 mm) overcome such aberrations, even when the specimen is imaged through an aqueous medium of 200-μm thickness.

For lenses that are designed to be used with a standard coverslip of 0.17-mm thickness (and $n_D = 1.515$), departure from standard thickness is not overly critical for objectives

TABLE 3 Color-coded Rings on Microscope Objectives

Color code (narrow colored ring located near the specimen end of objective)	
Black	Oil immersion
Orange	Glycerol immersion
White	Water immersion
Red	Special

Magnification color code (narrow band located further away from specimen than immersion code)	
Color	Magnification
Black	1, 1.25
Brown	2, 2.5
Red	4, 5
Yellow	10
Green	16, 20
Turquoise blue	25, 32
Light blue	40, 50
Cobalt (dark) blue	60, 63
White (cream)	100

with NA of 0.4 or less. However, for high-NA, nonhomogeneous immersion lenses, the problem becomes especially critical so that even a few micrometers' departure of the cover glass thickness degrades the image with *high-dry objectives* (i.e., nonimmersion objectives with high NA) of NA above 0.8 (Fig. 10). To compensate for such error, well-corrected, high-dry objectives are equipped with correction collars that adjust the spacing of their intermediate lens elements according to the thickness of the cover glass. Likewise, objective lenses that are made to be viewed through layers of silicon or plastic, or of different immersion media (e.g., water/glycerol/oil immersion lenses), are equipped with correction collars.

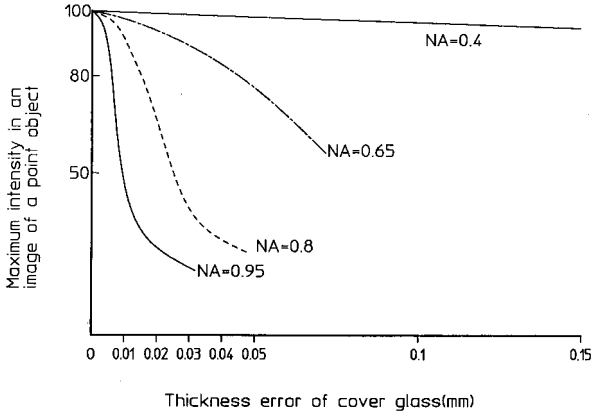

FIGURE 10 Calculated maximum intensity in the image of a point object versus the deviation of the coverglass thickness from the ideal thickness of 0.17 mm.[61]

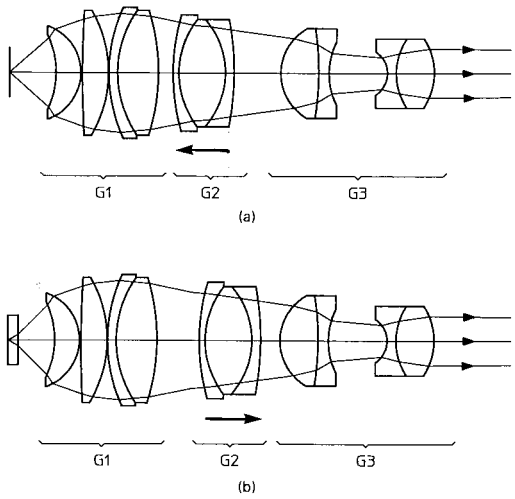

FIGURE 11 High-dry objective lens (60×/0.7 NA) equipped with a correction collar for (*a*) focusing at the surface or (*b*) through plane glass of up to 1.5-mm thickness. The lens group G_2 is moved forward to enhance the spherical and chromatic correction by G_1 and G_2 when focused on the surface, while it is moving backward to compensate for the presence of the glass layer when focusing deeper through the glass.[61] (U.S. Patent 4666256.)

The use of objective lenses with correction collars does, however, demand that the observer is experienced and alert enough to reset the collar using appropriate image criteria. Also, the focus tends to shift, and the image may wander, during adjustment of the correction collar. Figure 11 shows an example of a 60/0.7 objective lens equipped with a correction collar for focusing at the surface or through a cover glass of up to 1.5-mm thickness without altering the focal setting of the lens.

Tube Lengths and Tube Lenses for Which Microscope Objectives Are Corrected

For finite-focused ''biological'' objective lenses, most manufacturers have standardized the mechanical tube length to 160 mm (see Fig. 37). Most manufacturers use infinity focus for their metallurgical series (except Nikon uses a finite, 210-mm mechanical tube length). Carl Zeiss, Carl Zeiss Jena, Reichert and more recently Leica and Olympus have switched to infinity focus for both biological and metallurgical objectives.

For infinity-focused objective lenses, the rays emanating from a given object point are parallel between the objective and tube lens. Since the physical distance (D_p, Fig. 4) and optical path length between the objective and tube lens are not critical, optical components, such as compensators, analyzers, and beam splitters, can be inserted in this space without altering the objective's corrections. The tube lens focuses the parallel rays onto the intermediate image plane.

The magnification of an infinity-focused objective lens is calculated by dividing a *reference focal length* by the focal length of the objective lens. The reference focal lengths

TABLE 4 Reference Focal Lengths for Infinity-focused Objective Lenses

Leica	200 mm	B, M
Olympus	180 mm	B, M
Reichert	183.1 mm	B, M
Carl Zeiss	160 mm	B, M
Carl Zeiss Jena	250 mm*	B, M

B = biological, M = metallurgical.
* Subject to change in near future.

adopted by several manufacturers are listed in Table 4. For the ICS (Infinity Color-Corrected System optics) of Carl Zeiss, the reference focal length is fixed at 160 mm (both biological and metallographic) with the tube lens correcting the residual chromatic aberrations of the objective lenses. For current Carl Zeiss Jena infinity-corrected objectives (biological and metallographic), the objectives themselves are fully corrected for lateral and longitudinal chromatic aberrations, and tube lenses of various focal lengths are used to change magnification.

Working Distance

Microscope objectives are generally designed with a short free working distance, i.e., the distance from the front element of the objective lens to the surface of the cover glass or, in the case of lenses that are designed to be used without cover glass, to the specimen surface. For some applications, however, a long free working distance is indispensable, and special objectives are designed for such use despite the difficulty involved in achieving large numerical apertures and the needed degree of correction. Table 5 lists some objectives that provide extra-long working distances.

Field Size, Distortion

The diameter of the field in a microscope is expressed by the field-of-view number, or simply field number, which is the diameter of the field in millimeters measured in the intermediate image plane. The field size in the object plane is obviously the field number divided by the magnification of the objective. While the field number is often limited by

TABLE 5 Some Microscope Objectives with Long Working Distances Relative to NA

Manufacturer	Type	Mag/NA	FWD (mm)	CvrGl (mm)	Remarks*
Nikon	CF Plan Apo	4/0.20	15.0		TL = 160 mm
Leica	EF Achromat	4/0.12	24.0		Pol, TL = 160 mm
Zeiss	Plan Apo	5/0.16	12.2		ICO
Leica	Plan Fluotar	10/0.25	19.8		ICO, f.ref 200 mm, Pol
Leica	Plan	20/0.40	11.0	0	ICO, f.ref 200 mm
Olympus	Plan Achro	20/0.40	10.5	0–2	Corr, TL = 160 mm
Leica	Plan	40/0.60	6.8	0	ICO, f.ref 200 mm
Nikon	CF Plan	40/0.50	10.1	0.17	TL = 210 mm
Nikon	CF Plan	60/0.70	3.05	0.17	TL = 160 mm
Olympus	Neo S Plan	80/0.75	4.10	0	ICO, f.ref 180 mm
Olympus	Neo S Plan	100/0.80	3.20	0	ICO, f.ref 180 mm

FWD: free working distance; CvrGl: thickness of coverglass; TL: mechanical tube length; ICO: infinity-corrected objective, f.ref.: reference focal length.
* See Table 2 for other abbreviations.

the magnification and field stop of the ocular, there is clearly a limit that is also imposed by the design of the objective lens. In early microscope objectives, the maximum usable field diameter tended to be about 18 mm or considerably less, but with modern plan apochromats and other special flat field objectives, the maximum usable field can be as large as 28 mm or more. The maximum useful field number of objective lenses, while available from the manufacturers, is unfortunately not commonly listed in microscope catalogs. Acknowledging that these figures depend on proper combination with specific tube lenses and oculars, we should encourage listing of such data together with, for example, UV transmission characteristics (e.g., as the wavelength at which the transmission drops to 50 percent, or some other agreed upon fraction).

Design of Modern Microscope Objectives

Unlike earlier objective lenses in which the reduction of secondary chromatic aberration or curvature of field were not stressed, modern microscope objectives that do correct for these errors over a wide field tend to be very complex. Here we shall examine two examples, the first a 60/1.40 Plan Apochromat oil-immersion lens from Nikon (Fig. 12).

Starting with the hyperhemisphere at the front end (left side of figure) of the objective, this aplanatic element is designed to fulfill Abbe's sine condition in order to minimize off-axis spherical aberration and coma, while providing approximately half the total magnifying power of the objective (Fig. 13). In earlier designs, the hyperhemisphere has been made with as small a radius as possible in order to maximize its magnifying power and to minimize its spherical and chromatic aberrations, since these aberrations increase proportionally with the focal length of the lens. Modern demands for larger field size and reduced curvature of field, however, introduce a conflicting requirement, namely, the need to maintain as large a radius as practical in order to minimize the hyperhemisphere's contribution to the Petzval sum (the algebraic sum of the positive and negative curvatures multiplied by the refractive indices of the lens elements). The hyperhemisphere in these Plan Apochromats is made with a high-index, low-dispersion material to compensate for the greater radius. Additionally, a negative meniscus is generated in the front surface of the hyperhemisphere to which is cemented a minute, plano-convex lens. The negative curvature in the hyperhemisphere contributes to the reduction of the Petzval sum. At the same time the minute plano-convex lens protects the material of the hyperhemisphere which is less resistant to weathering. Index matching between the minute plano-convex lens and immersion oil eliminates or minimizes the refraction and reflection at the lens-oil interface and provides maximum transmission of the all-important high-NA rays into the objective lens. The index matching also reduces the influence of manufacturing errors of this minute lens element on the performance of the objective.

The low-dispersion-glass singlet behind the aplanatic hyperhemisphere further reduces the cone angle of the rays entering the doublets that follow, allowing these and the subsequent lenses to concentrate on correcting axial and lateral chromatic aberration as well as curvature of field. These errors, as well as residual spherical aberrations, are corrected by inclusion of low-dispersion positive and high-dispersion negative lens elements, use of thick-lens elements, appropriate placement of positive and negative lens

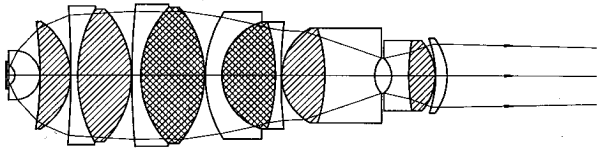

FIGURE 12 Design of Nikon Plan Apochromat oil-immersion objective with 60× magnification and 1.40 NA.[61]

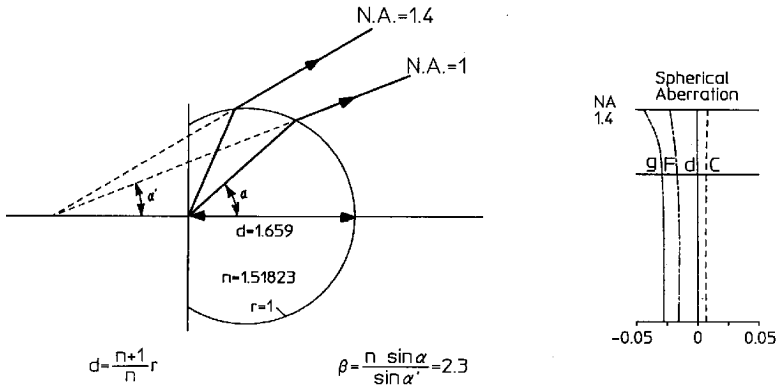

FIGURE 13 Aplanatic condition of the hyperhemisphere placed at the front end of an oil-immersion objective. The front lens has the same refractive index as the coverglass and immersion oil. The aplanatic condition describes the necessary relationship between refractive index n, distance d between object and spherical surface, and radius r of the spherical surface, in order to make all rays emanating from an object point on the axis leave the hemispherical surface after refraction without introducing spherical aberration. On the right, the small amount of spherical aberration and deviation from the ideal focus point of the hyperhemisphere is shown for different wavelengths (C = 656 nm, d = 588 nm, F = 486 nm, g = 436 nm).[61]

curvatures, and through extensive ray tracing. Near the exit pupil, the height of the ray paths through the concave surfaces is reduced in order to generate additional negative values that minimize the Petzval sum (to complement the inadequate negative contribution made by the concave surface in the hyperhemisphere), so that field flatness can be improved without overly reducing the objective lens' magnifying power or adding to its spherical aberration.

In reality, the Petzval sum of the objective as a whole is made somewhat negative in order to compensate for the inevitable positive Petzval sum contributed by the ocular. Thus, the image at the intermediate image surface, especially the sagittal surface of modern objectives, bows away from the object. Unless the image area is relatively small, one needs to use specified oculars in order to attain maximum field flatness combined with optimum correction otherwise.

Unlike earlier objective lenses (Figs. 2*a* to 2*d*) whose design did not appreciably vary from one manufacturer to another, the design of lenses in modern microscope objectives can vary considerably. For example, compare the Nikon Chrome Free 60/1.4 Plan Apo objective discussed above and the Zeiss Infinity Color-Corrected Systems 63/1.4 Plan Apo objective in Fig. 14. Both are excellent, state-of-the-art lenses. But in addition to general design philosophy, including the decision to avoid or to use tube lenses to achieve full chromatic corrections, other factors such as choice of optical elements with special dispersion characteristics; degrees of UV transmission; freedom from fluorescence, birefringence, aging loss of transmittance, etc., all affect the arrangement of choice.

While a modern research-grade microscope is corrected to keep the aberrations from spreading the image of a point source beyond the Airy disk, geometrical distortion of the image formed by microscope objectives tends not to be as well-corrected (e.g., compared to photographic objectives at the same picture angle). Thus, in objectives for biological use, pincushion distortions of up to 1 percent may be present. However, in objectives that are designed for imaging semiconductors, the distortion may be as low as 0.1 percent and they can be considered nearly distortion-free. To reduce stray light and flare, modern microscope objectives contain lens elements with carefully tuned, antireflection coatings,

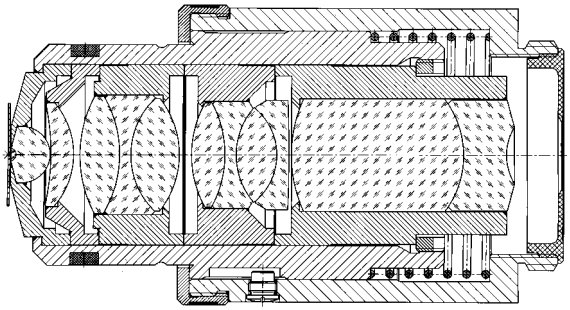

FIGURE 14 Carl Zeiss Infinity Color-Corrected 63/1.4 Plan Apo objective. (*Courtesy of E. Keller, Carl Zeiss, N.Y.*)

and lens curvatures are selected to minimize ghost images arising from multiple reflections.

Given the sophisticated design to provide a wide flat field, with spherical aberrations corrected over a broad wavelength range, and with low longitudinal as well as chromatic aberrations corrected at high NA, the aberration curves of these modern microscope objectives no longer remain simple cubic curves, but turn into complex combinations of higher-order curves (Fig. 15).

Oculars

As conventionally illustrated, the ocular in a light microscope further magnifies the primary (intermediate) image formed by the objective lens (Figs. 3 and 4). The ocular can also be viewed as the front elements of a macro (relay) lens system made up of the ocular plus the refractive elements of the viewer's eye (Fig. 5*a*) or a video or photographic camera lens. Special video and photo oculars combine these functions of the ocular plus the video or photo lenses into single units.

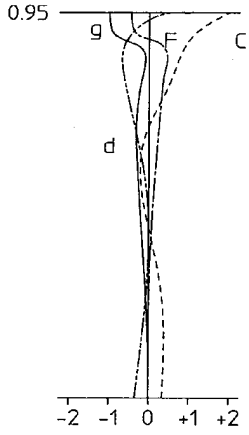

FIGURE 15 Spherical aberration of a highly corrected modern microscope objective with a high numerical aperture.[61]

The intermediate image plane (that lies between the lenses in many ocular types or precedes the lens elements in the Ramsden-type oculars), or its conjugate plane, is used to place field limiting stops, iris diaphragms, reticles, micrometer scales, comparator beam splitters, etc., that need to appear in the same focal plane as the specimen.

The Ramsden disk, the exit pupil of the objective lens imaged by the ocular, generally appears a short distance above the ocular (Fig. 5*b*). Since the Ramsden disk should lie in the observer's pupil, special high-eye-point oculars are provided for the benefit of observers wearing corrective eye glasses (especially those for astigmatism). High-eye-point oculars are also used for inserting beam-deviating devices (such as the scanning mirrors in laser scanning confocal microscopes) or aperture-modifying devices (such as aperture occluders for stereo viewing through single objective binocular microscopes[6]).

The magnification of an ocular is defined as 25 cm divided by the ocular's focal length. On the ocular, the magnification and field number are inscribed (e.g., as 10×/20, meaning 10-power or 25-mm focal length with a field of view of 20-mm diameter), together with manufacturer's name and special attributes of the ocular such as chromatic-aberration-free (CF), wide-field (W, WF, EWF), plan (P, Pl), compensation (Comp, C, K), high-eye-point (H, picture of glasses), with cross hair and orientation stub for crystallography (pol), projection (pro), photographic (photo), video (TV), etc. Also, special oculars provide larger and flatter fields of view (designated Wide Field, Extra Wide Field, Plan, Periplan, Hyperplan, etc., some with field numbers ranging up to 28 mm).

Compared to microscope objective lenses, fewer design standards have been adopted and fewer standard abbreviations are used to designate the performance or function of the oculars. Two physical parameters of the oculars have, however, become more or less standardized. The outside diameter of the ocular is either 23.2 mm or 30.0 mm, and the reference distance, or the parafocalizing distance of the ocular (i.e., the location of the intermediate image plane below the flange of the ocular) is now generally set to 10 mm.

In the past, oculars with wide ranges of incremental magnifications were provided to adjust the total image magnification of the microscope, but this practice is now replaced by the use of much fewer, better-corrected oculars coupled with a telan magnification changer in the microscope's body tube, or a zoom projection ocular.

Factors affecting choice of ocular focal length and magnification include optimizing the microscope total magnification and image resolution to match the MTF characteristics of the detector and to adjust the available field coverage. In video-enhanced fluorescence, DIC, polarizing, dark field, etc., microscopy, the total magnification often needs to be raised beyond the classical ''empty magnification'' limit, in order to be able to visualize minute objects whose diameters lie well below the limit of microscope resolution.[6] However, depending on the MTF characteristics, sensitivity, and total pixels available in the sensor, conflicts may arise between the need for greater magnification, image brightness, and field coverage. To optimize the total image magnification, fine trimming of the ocular magnification may be needed, in addition to choosing an objective with the appropriate magnification and NA-to-magnification ratio. Zoom oculars are especially suited for fine-tuning the magnification to optimize S/N ratio and image integration time in video microscopy. For very low light level images, e.g., in photon-counting imaging, ocular magnifications of less than one may be needed in order to sufficiently elevate the S/N ratio, albeit at a sacrifice to spatial resolution.

In addition to adjusting image magnification and placing the microscope's exit pupil at a convenient location, the ocular compensates for the aberrations that have not been adequately corrected in the objective and tube lens. Huygens oculars combined with lower-power achromatic objectives, and compensating oculars combined with higher-NA achromatic and apochromatic objectives, correct for lateral chromatic aberration. Some higher-NA achromatic objectives are purposely designed to provide residual aberrations (including field curvature) that are similar to those in the apochromats, so that the same compensation oculars can be used to compensate for both types of objectives.

Certain classes of modern objectives are sufficiently well corrected to require minimum

compensatory correction by the oculars. For example, the Nikon CF objectives and the current Zeiss Jena objectives are designed to produce sufficiently well-corrected intermediate images so that the oculars themselves also are made independently free of lateral and longitudinal chromatic and some spherical aberrations. Regardless of the degree of correction relegated to the ocular, modern microscopes provide images with color corrections, fields of view, and flatness of field much superior to earlier models.

17.5 CONTRAST GENERATION

In microscopy, the generation of adequate and meaningful contrast is as important as providing the needed resolution. Many specimens are transparent and differ from their surroundings only in slight differences of refractive index, reflectance, or birefringence. Most objects that are black or show clear color when reasonably thick become transparent or colorless when their thickness is reduced to a few tenths of a micrometer (since absorption varies exponentially with thickness). Additionally, the specimen is illuminated at large cone angles to maximize resolution under the microscope, thus reducing the shadows and other contrast cues that aid detection of objects in macroscopic imaging. Furthermore, contrast is reduced at high spatial frequency because of an inherent fall-off of the contrast transfer function.

Many modes of contrast generation are used in microscopy partly to overcome these limitations and partly to measure, or detect, selected optical characteristics of the specimen. Thus, in addition to simply raising contrast to make an object visible, the introduction of contrast that reflects a specific physical or chemical characteristic of the specimen may provide particularly important information.

As a quantitative measure of expected contrast generation as functions of spatial frequencies, the modulation transfer functions (MTFs, of sinusoidal gratings) can be calculated theoretically for various contrast-generating modes assuming ideal lenses (Figs. 16 and 17[16]), or on the basis of measured point or line spread functions.[17] Alternatively, the contrast transfer function (CTF, of square wave gratings) can be measured directly using test targets made by electron lithography (Fig. 18).

In the remainder of this section, we survey microscope optical systems according to their modes of contrast generation.

Bright Field

Whether on an upright or inverted microscope, bright field is the prototypic illumination mode in microscopy (Fig. 5). In transmission bright-field illumination, image contrast commonly arises from absorption by stained objects, pigments, metal particles, etc., that possess exceptionally high extinction coefficients, or in the case of transparent objects, from the Becke lines introduced by refraction at object boundaries that are slightly out of focus. (The dark Becke line, which is used for immersion determination of refractive index of particles,[18] surrounds, or lies just inside, a boundary with a sharp gradient of refractive index when the boundary is slightly above or below focus. The Becke line disappears altogether when a thin boundary is exactly in focus.)

To gain additional contrast, especially in bright-field microscopy, the condenser NA is commonly reduced by closing down its iris diaphragm. This practice results in loss of resolution and superimposition of diffraction rings, Becke lines, and other undesirable optical effects originating from regions of the specimen that are not exactly in focus. The various modes of optical contrast enhancement discussed in following sections obviate this

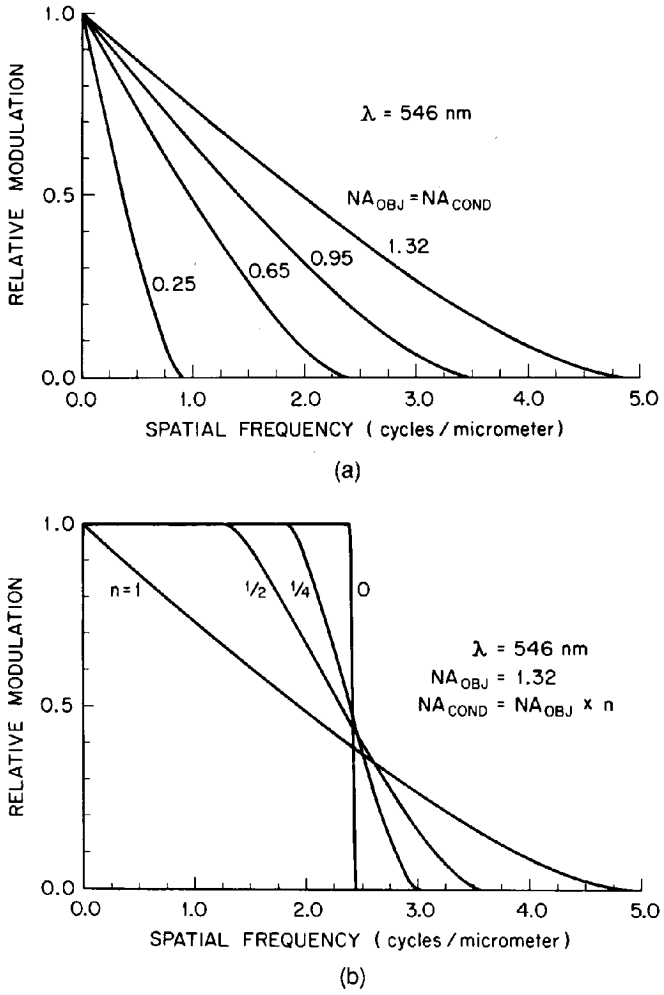

FIGURE 16 Modulation transfer function (MTF) curves for microscope lenses, calculated for periodic specimens in focus: (*a*) each curve represents a different numerical aperture (NA), which is the same for the objective and condenser lens in these curves. (*b*) These MTF curves all represent an objective lens of 1.32 NA, but with different condenser NAs; the conditions are otherwise the same as in (*a*). (*Courtesy of Dr. G. W. Ellis.*)[6]

limitation and provide images with improved lateral and axial resolution as well as improved contrast.

Before the advent of phase contrast and DIC microscopy, oblique illumination (that can be attained by off-centering a partially closed condenser iris diaphragm) was used to generate contrast of transparent objects. While this particular approach suffered from the problems listed in the previous paragraph, combination of oblique illumination at large condenser NA with video contrast enhancement proves to be an effective method for generating DIC-like thin optical sections.[19]

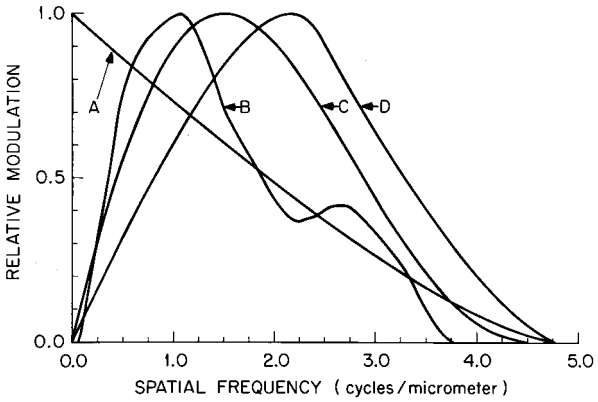

FIGURE 17 Modulation transfer function curves calculated for different modes of microscope contrast generation. A = bright field, B = phase contrast, C = differential interference contrast, and D = single-sideband edge enhancement. The curves are plotted with their peak modulation normalized to 1.0. (*Courtesy of Dr. G. W. Ellis.*)[6]

In reflection bright-field microscopy, the image is formed by the reflected or backscattered light of the specimen which is illuminated through the objective (see the sect. on "Epi-illumination"). Reflection contrast is used primarily for opaque and thick samples, especially for metals and semiconductors. Reflection contrast is also finding increasing applications in autoradiography and in correlative light and electron microscopy for detecting the distribution of colloidal gold particles that are conjugated to antibodies and other selective indicators.

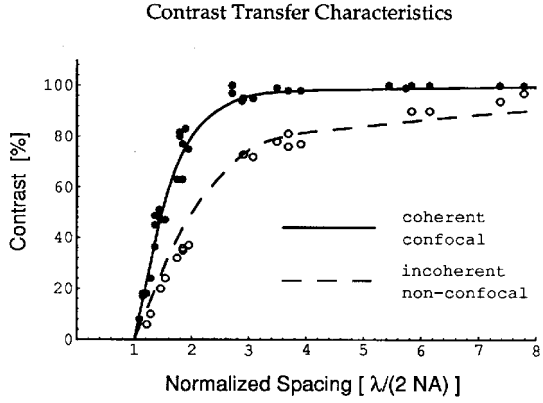

FIGURE 18 Measured contrast transfer values plotted as a function of spatial period in Airy disk diameter units, to normalize the values measured with different lenses and wavelengths. Data points were obtained with a laser spot scan microscope operating in the confocal reflection mode (*solid points*) and the nonconfocal transmission mode (*circles*). Curves are calculated contrast transfer values for the coherent confocal and the incoherent nonconfocal imaging mode.[62]

Total frustrated reflection microscopy[20] generates contrast due to objects that are present in a low-refractive-index medium located within the evanescent wave that extends only a few wavelengths' distance from the microscope coverslip surface. Regions of the specimen whose refractive index differs from its milieu produce interference fringes whose contrast sensitively reflects the refractive index difference and distance from the coverslip surface.

Dark Field

In dark field microscopy the illuminating beam is prevented from entering the image-forming ray paths. The background of the field is dark, and only light scattered by optical discontinuities in the specimen is designed to appear in the image as bright lines or dots. Thus, contrast can become extremely high, and diffraction images can be detected as bright points or lines even when the diameter of the scattering object becomes vanishingly small compared to the microscope's limit of resolution.[4,12,14]

For small objects that are not obscured by other light-scattering particles (a condition rather difficult to achieve) and are free in a fluid substrate, Brownian motion of the object and the time constant and sensitivity of the detector, rather than the object's absolute size, are more likely to set a lower limit to the size of the object that can be clearly visualized with dark field microscopy.

Phase Contrast and Other Aperture-modifying Contrast Modes

Microscopic objects, distinguished from their surround only by a difference of refractive index, lose their Becke line and disappear altogether when brought exactly into focus. Nevertheless, light diffracted by the small object still suffers a $\lambda/4$ phase shift relative to the undeviated background wave by the very act of being scattered (by a nonabsorbing object; the phase shift upon scattering by an absorbing object is $\lambda/2$[21]). As shown in Fig. 19, light s scattered by the small object and the undeviated light u, both originating from a common small point A of the condenser aperture, traverse different regions of the objective lens aperture. At the objective aperture, the undeviated light traverses only point B that is conjugate to A, while the scattered light passes those regions of the aperture defined by the spatial periods of the object.

Since light waves s and u arise from the same points in object space but traverse regions that are spatially separated in the objective aperture plane, a *phase plate* introduced in that plane can be used to modify the relative phase and amplitudes of those two waves. The phase plate is configured to subtract (or add) a $\lambda/4$ phase to u relative to s so as to introduce a $\lambda/2$ (or zero) phase difference between the two and, in addition, to reduce the amplitude of the u wave so that it approximates that of the s wave. Thus, when the two waves come to focus together in the image plane, they interfere destructively or constructively to produce a darker or brighter, in-focus image of the small, transparent object against a dark gray background.

As generally implemented, an annulus replaces the pinhole in the condenser aperture, and a complementary phase ring in the objective aperture plane or its conjugates (covering a somewhat larger area than the undisturbed image of the annulus in order to handle the u waves displaced by out-of-focus irregularities in the specimen) replaces the simple phase disk.

In the Polanret system, the phase retardation and effective absorbance of the phase ring can be modified by use of polarization optical components so that the optical path difference of a moderately small object can be measured by seeking the darkest setting of

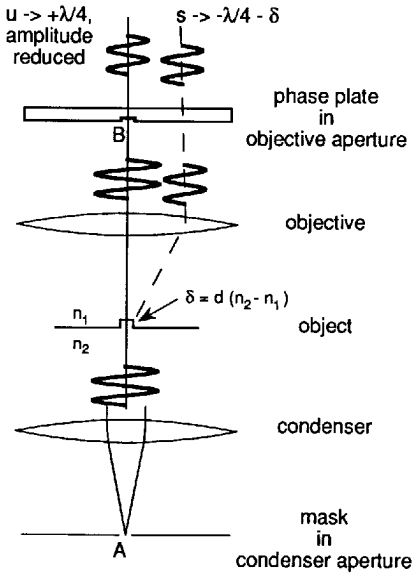

FIGURE 19 Optical principle of phase contrast microscopy illustrating the phase relationships between waves of the light *s* scattered by the specimen and the undeviated light *u* (see text).

the object.[22] Similarly, the Polanret system can be used to accentuate color or low contrast due to slight absorption by the object.

Several modes of microscopy, including phase contrast, specifically take advantage of the facts that (1) the condenser and objective lens apertures are conjugate planes, (2) the illuminating beam arising out of each point of the condenser aperture is variously deviated by the specimen structure according to its spatial frequency, and (3) the objective aperture is the Fourier plane.

In modulation contrast microscopy, the condenser aperture contains a slit mask with the slit placed towards the edge of the aperture. The objective aperture holds a second, complementary mask, called a modulator, which consists of two parts (Fig. 20). The dark part covers the smaller sector to one side of the projected slit and the gray part covers the slit area. The objective mask thus attenuates the zero-order light undeviated by the specimen and removes the light diffracted by the specimen to one side of the zero-order beam. The light deviated by specimen structure away from the dark sector of the mask passes unchanged, while the light deviated towards the dark sector is blocked. Thus, the image becomes shadow-cast, similar in appearance to differential interference contrast (DIC) that reflects gradients of refractive indices or of optical path differences in the specimen.

In single sideband edge enhancement (SSBEE) microscopy, a halfstop is placed at the front focal plane of the condenser to occlude one half of the condenser aperture. A complementary spatial filter in the objective aperture attenuates the undeviated beam and controls its phase displacement by adjustable amounts relative to the light scattered by the object into the aperture region obscured by the condenser halfstop (single sideband[23]). Thus, we again acquire an image similar in appearance to DIC, but which, unlike DIC, does not require polarization optical elements to sandwich the specimen, and thus can be used to detect very minute anisotropies of refractive index at high resolution. The SSBEE

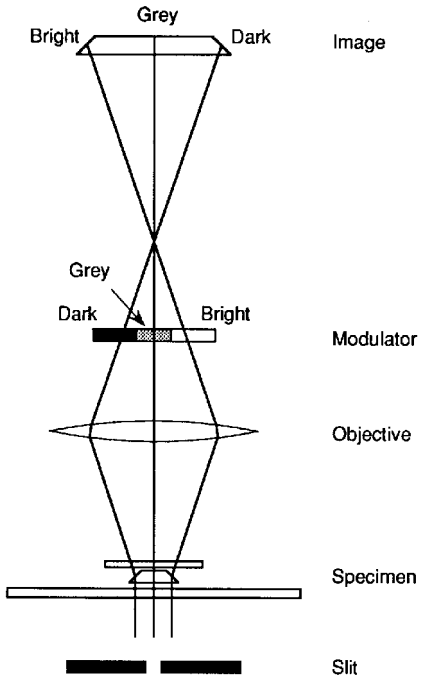

FIGURE 20 Schematic diagram indicating regions of the modulator that modify light from phase gradients in the object to enhance contrast.[63]

system takes advantage of the fact that one needs to capture only one of the two beams (sidebands) deviated by diffraction in order to gain the information regarding the spatial frequency in the specimen that gives rise to that particular diffraction angle.

Polarizing

The polarizing microscope generally differs from a standard transilluminating microscope by the addition of a polarizer below the condenser; a compensator slot and analyzer above the objective lens; strain-free optics; a graduated, revolving stage; centrable lens mounts; cross hairs in the ocular aligned parallel or at 45° to the polarizer axes; and a focusable Bertrand lens that can be inserted for conoscopic observation of interference patterns at the back aperture of the objective lens. In addition, the front element of the condenser can be swung into place for higher-NA conoscopic observations or swung out for low-NA orthoscopic observations of larger field areas.

Calcite polarizing prisms (which introduce astigmatism to all but collimated rays) have mostly been replaced in recent years by dichroic polarizing filters. The polarizing filters are thin and cost very much less, although inferior in transmittance and extinction compared to high-quality polarizing prisms. The lower transmittance through a pair of polarizing filters is especially detracting in high-extinction polarized light or DIC microscopy, since only a small fraction of light originating from a low birefringence or path difference in the sample reaches the observer's eyes or the video detector.

With standard polarizing microscopes, one can image and measure polarization optical parameters[18,24] on objects which are larger than a few micrometers and which introduce

retardances greater than several tens of nanometers. However, as the dimension of the object or magnitude of retardance decrease below these ranges, one needs to use special techniques or devices for detecting and measuring birefringence or even for generating a reliable image with high-NA lenses.

The basic ingredients that are needed to detect low levels of birefringence (retardance $\leq$10 nm) are high-extinction optics, use of low-retardance compensator, light source with high irradiance, and high-sensitivity detector (e.g., dark adaptation for visual observation and measurements). These needs can be understood from the following formula:

$$I = I_p(\sin^2(R/2) + 1/\mathrm{EF}) \tag{10}$$

where I is the irradiance of the specimen with a retardance of R (radians), L_p is the irradiance of the field when the polarizer and analyzer axes are parallel (i.e., maximum transmission), and the extinction factor $\mathrm{EF} = I_p/I_c$, where I_c is the irradiance when $R = 0$.[25] For example, when the specimen retardance is 2 nm at a wavelength of 555 nm, then $R = 2\pi \times 2/555$, $\sin^2(R/2) = 1 \times 10^{-4}$. In other words, the specimen has only twice the irradiance as the background even when EF is as large as 10^4. The field is also only 10^{-4} of its irradiance compared to when the polarizer and analyzer axes are set parallel, or when observing a specimen with a full wavelength retardance between crossed polarizers. Inclusion of the compensator adds a bias compensation that increases contrast (the irradiance of the specimen relative to that of the background field) as well as field irradiance. An intense light source and dark adaptation of the observer also help shift the field and specimen irradiance into ranges that reduce the contrast threshold of the eye (or improve the S/N ratio of a photoelectric detector or for photography).

The EF of a polarizing microscope rapidly drops (to as low as 2×10^2 when $\mathrm{NA_{obj}} = \mathrm{NA_{cond}} = 1.25$) as the NA of the system is raised, even with polarizer $\mathrm{EF} > 10^5$, and using carefully selected objective and condenser lenses that are free from strain birefringence or birefringent inclusions. The loss of EF originates from the rotation of polarization plane and birefringence that results from differential transmission of the P and S components at the optical interfaces. The depolarization results in four bright quadrants separated by a dark cross that is seen conoscopically for crossed polarizers in the absence of a specimen. The depolarization also gives rise to anomalous diffraction, and a four-leaved clover pattern replaces the Airy disk or each weakly birefringent image point[26] (see Ref. 6, Fig. III-23).

Anomalous diffraction and the loss of EF at high NAs are both eliminated or drastically reduced by introducing polarization rectifiers (Fig. 21). The rectifier corrects for the differential P vs. S transmission loss regardless of their absolute values, thus resulting in a uniformly high extinction for the full aperture (Fig. 22). The resulting uniform aperture function accounts for the absence of anomalous diffraction in a rectified system.[27] The image improvement achieved with rectifiers in a polarizing microscope is demonstrated in Fig. 23.

Interference

While all modes of contrast generation in light microscopy in fact depend on interference phenomena, a group of instruments is nevertheless known separately as interference microscopes. These microscopes form part of an interferometer, or contain an interferometer, that allows direct measurements of optical path difference (or generaton of contrast) based on inteference between the waves passing the specimen and a reference wave.

Among the many designs that have been manufactured or proposed, interference microscopes can be classified into three major groups: (1) the Mach-Zehnder type where two complete sets of microscope optics are placed, one in each arm of a Mach-Zehnder interferometer; (2) the beam-shearing type in which the reference wave is generated by

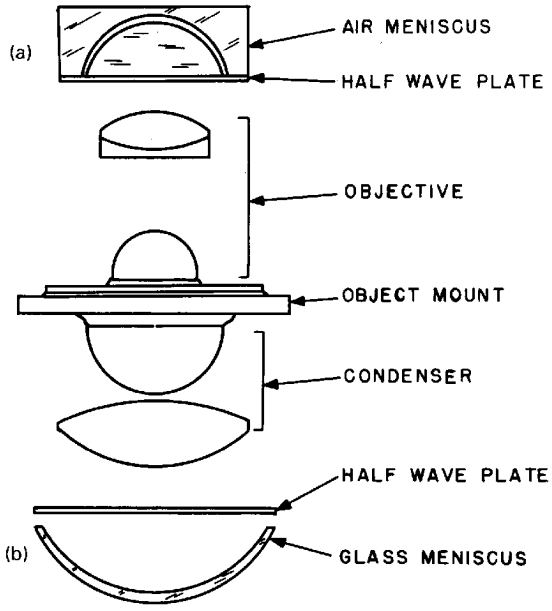

FIGURE 21 Arrangement of polarization rectifiers. Rectifiers are placed above the objective *A,* below the condenser *B*, or at both *A* and *B*. The glass or air meniscus introduces additional rotation to each beam of light which equals the amount introduced by the lenses and the specimen slide. The sense of rotation is, however, reversed by the half-wave plate so rectification is achieved over the whole aperture.[64]

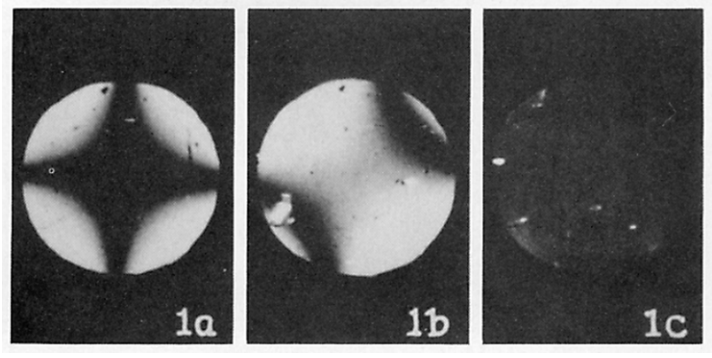

FIGURE 22 Appearance of the back aperture of a 1.25-NA strain-free objective with and without rectifiers. The condenser, which is identical with the objective, is used at full aperture. (*a*) Crossed polarizers, no rectifier; (*b*) polarizer turned 2°, no rectifier; (*c*) crossed polarizers, with rectifiers in both condenser and objective. Photographs were given identical exposures.[64]

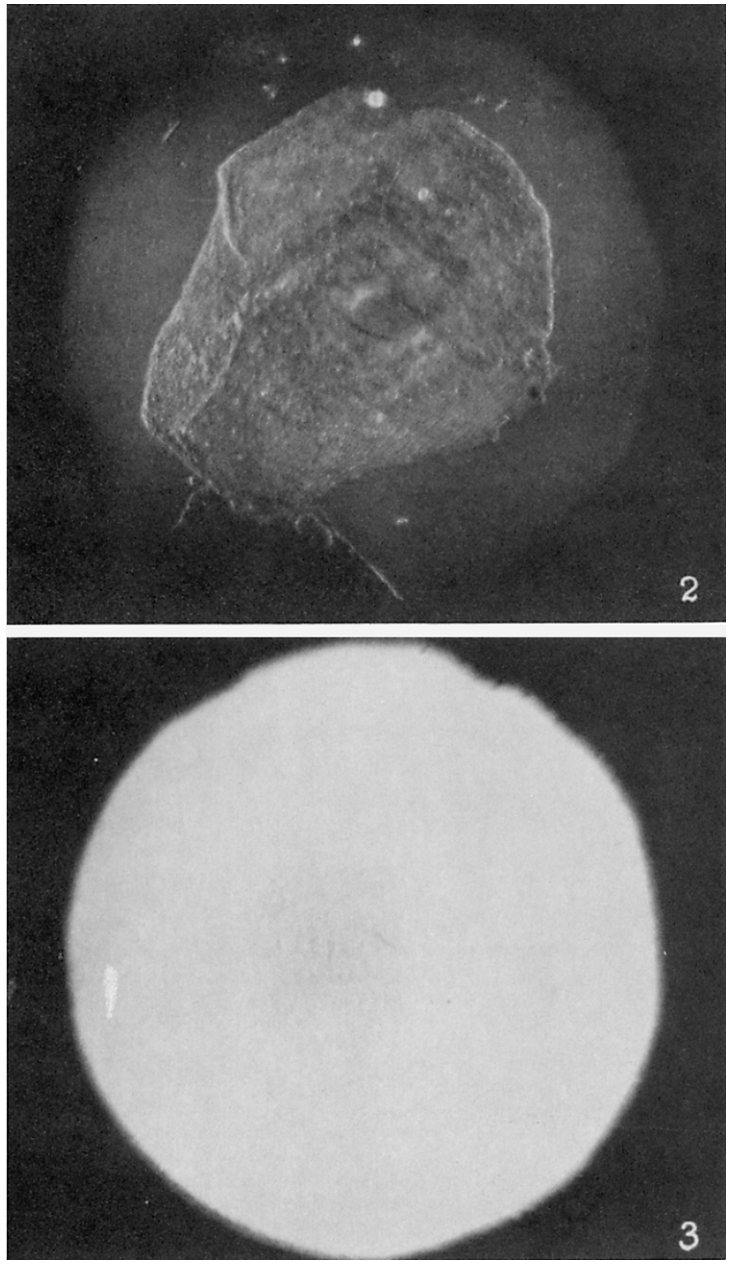

FIGURE 23 (*Top*) Photograph of an epithelial cell from a human mouth taken with a 43×/0.85-NA strain-free objective and a 43×/0.63 strain-free condenser equipped with a rectifier. Polarizers crossed, 1-nm background retardation (horizontal image width approx. 150 μm). (*Bottom*) Identical to *top* but without a rectifier. Notice the brighter background and the total lack of detail and contrast in the image.[64]

displacing a beam laterally within the field of a single microscope; and (3) the Mirau type in which the reference wave is focused to a different level than the specimen plane, again in a single microscope.

The Mach-Zehnder type (Fig. 24), while straightforward in principle, requires close

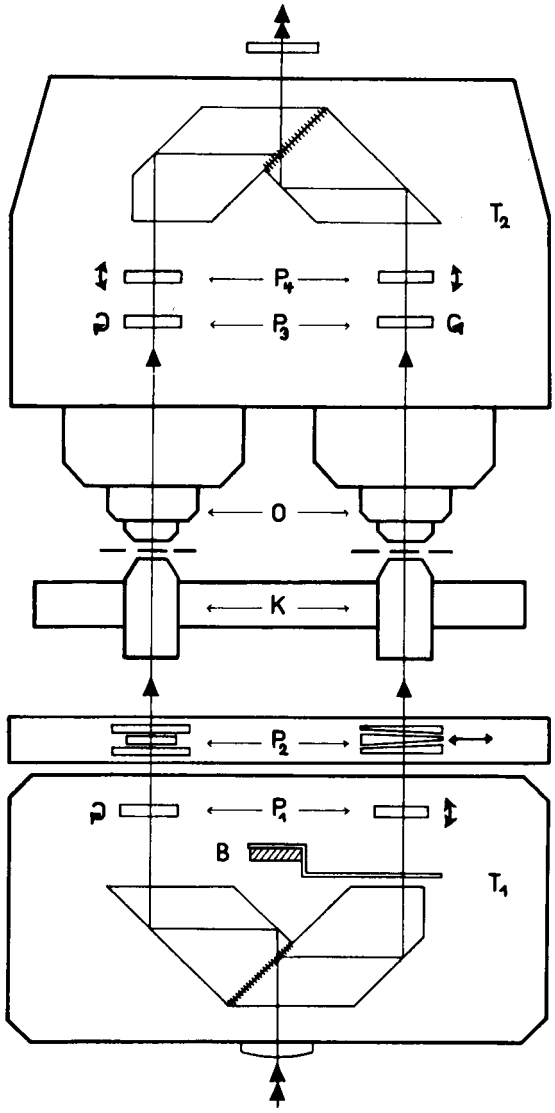

FIGURE 24 Mach-Zehnder type interference microscope with two complete sets of microscope optics, one in each arm of a Mach-Zehnder interferometer. The compensators P_1, P_2, P_3, and P_4 introduced into the beam path permit optimum contrast setting and adjust for any variation of the interference picture. (*Reproduced from E. Leitz Inc., Catalog No. 500-101 Interference Systems, 1972.*)

matching of the optics in the two interferometer arms and a mechanical design that provides exceptional precision and stability. Thus, in addition to using one of the matched pairs of objectives and the corresponding matched pairs of condensers that are mounted on special sliders, and inserting a blank slide (that is similar to the specimen-containing slide) into the reference path, for each specimen change, one needs to carefully adjust the built-in beam deviators, path equalizers, and wedge components to correct for deviation of the beam paths and to precisely equalize the optical paths through the two microscopes. While unfortunately no longer manufactured, this type of microscope permits precise interferometric measurements of microscopic objects both in the uniform field mode and the fringe displacement mode, and can even be used to generate holograms (Dr. G. W. Ellis, personal communication).

Several variations exist of the two latter types of interference microscopes.[4,28] Many designs use a polarizer, polarized beam splitters, and a half-wave plate sandwiching the specimen to generate and recombine the two beams, and a quarter-wave plate and graduated rotatable analyzer to measure optical path difference (Fig. 25). Depending on the crystal arrangements in the polarizing beam splitter, the reference beam is either laterally displaced in the field or at a different focal level from the primary imaging beam. In this type of interference microscope, one needs to be wary of ghost images introduced by the dual beam paths. Some interference microscopes for noncontact surface profiling employ objectives according to the design of Mirau (Fig. 26).

With all the interference microscopes, both monochromatic and white light illumination can be used. Monochromatic illumination allows precise measurement of optical path difference and determination of the dry mass (i.e., reduced weight) of the specimen if its thickness is known or can be calibrated, e.g., by altering the refractive index of the immersion medium.[29,30] White light illumination allows determination of the order of the fringes or interference colors. In uniform field mode, the interference color has been used as a method of contrast generation, but such use of the interference microscope was soon replaced by DIC which can be used with higher-NA lenses and thus provide greater image resolution.

Differential Interference Contrast (DIC)

Differential interference contrast (DIC) microscopy provides a monochromatic shadow-cast image that effectively displays the gradient of optical paths for both low and high spatial frequencies. Those regions of the specimen where the optical paths increase along a reference direction appear brighter (or darker), while those regions where the path differences decrease appear in reverse contrast. Image contrast is greater the steeper the gradient of path difference. Thus, a spherical object with higher index than its surround would appear to be highlighted on one side with shadows cast on the other side. Objects whose refractive index is less than the surround appear with reverse shadow-cast appearance as though it were a depression. Very thin filaments or sharp interfaces likewise appear shadow-cast and with good contrast, even when their diameter or separation falls way below the limit of resolution of the optical system.

DIC is basically a beam-shearing interference contrast system in which the reference beam is sheared by a minuscule amount, generally by somewhat less than the diameter of the Airy disk. The basic system devised by Smith[31] is a modified polarizing microscope to which two Wollaston prisms are added, one at the front focal plane of the condenser and the other at the back focal plane of the objective lens (Fig. 27). The condenser Wollaston converts each ray illuminating the specimen into two, slightly displaced, parallel beams that are orthogonally polarized relative to each other. In the second Wollaston prism above the objective, the two beams become recombined again.

The phase difference between the two beams, introduced by a gradient of thickness or refractive index in the specimen, results in elliptical polarization for the recombined beam

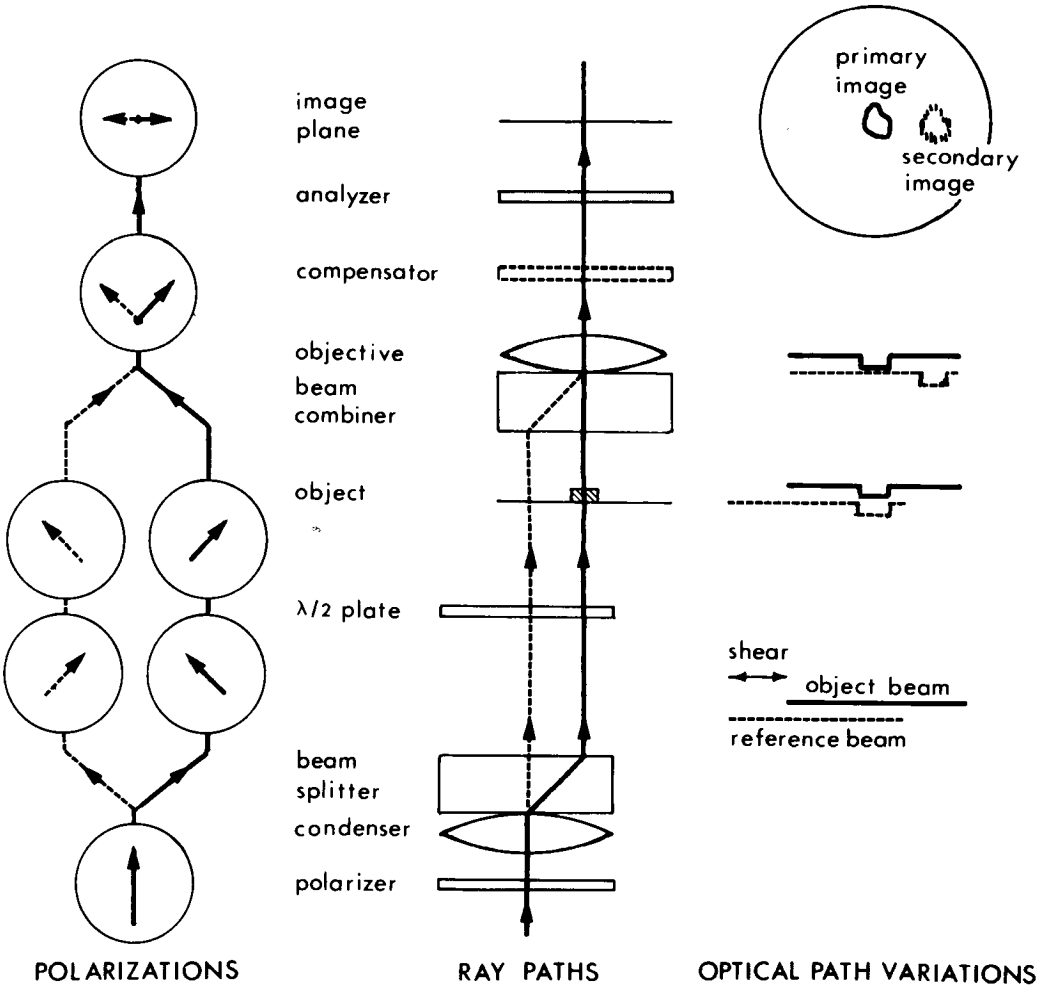

FIGURE 25 Jamin-Lebedeff interferometer microscope. The reference and object beam are polarized orthogonally by the birefringent beam splitter and are separated by a sizeable fraction of the field diameter. The half-wave plate switches the polarization of the two beams so that the second birefringent plate in front of the objective serves as a beam combiner. The compensator (quarter-wave plate and graduated rotatable analyzer) serves to measure optical path differences between reference and object beam.[65]

that leaves the second Wollaston. A deSenarmont compensator (a quarter-wave plate in extinction position and rotatable analyzer) is placed above the second Wollaston to extinguish light that has suffered a particular phase shift relative to the other beam. Alternatively, the quarter-wave plate can be inserted between a rotatable polarizer and the condenser Wollaston prism.

In medium- to high-power objective lenses, the back focal plane is usually inside the lens system and therefore not available for insertion of a Wollaston prism. To avoid this problem, Nomarski[32] introduced a modification of the Wollaston prism that can be placed outside of the objective lens (Fig. 28). By using crystal wedges with appropriately oriented axes, the Nomarski prism recombines the two beams that were separated by the

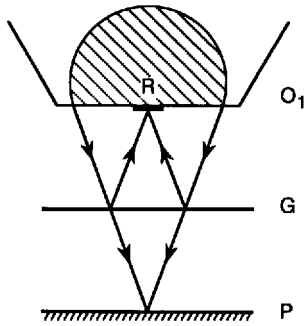

FIGURE 26 Mirau's interference microscope. The incident light beam, emerging from the objective O_1, is split in two parts in the semireflective plate G. One part is transmitted to the object P and the other is reflected to the reference area R extending over a small portion of the objective front surface. The wavefronts reflected by R and P are recombined at G to produce the interference pattern.[4]

condenser Wollaston as though a regular Wollaston prism were located in the proper plane in the objective lens. Regions of the specimen with selected phase shifts are compensated by translating the Nomarski prism. A second modification introduced by Nomarski (and for a while adopted by Nikon) uses a single crystal in place of the condenser Wollaston and a three-part prism in place of the Nomarski prism described above.[33]

Fluorescence

Fluorescence microscopy is one of the few modes of microscopy in which the illuminating wavelength differs from that of the emitted. In early designs, the exciting waves were prevented from contaminating the fluorescence image by a combination of (1) special illumination (such as the use of a dark-field condenser) that prevented the direct rays from entering the objective lens, and (2) the use of a barrier filter. The barrier filter absorbs the exciting light while transmitting much of the longer fluorescence wavelengths. (*Note*: For every fluorochrome, the longer wavelength portion of the absorption curve, i.e., the excitation wavelengths, overlaps with the shorter wavelength tail of its fluorescence emission curve.)

Today most fluorescence microscopes (or attachments) use epi-illumination incorporating interchangeable filter cubes (after Ploem, see Fig. 30) that are matched to the fluorochrome. The filter cube is placed in the collimated beam between the objective and a tube lens, at the intersection of the microscope axis and that of the excitation illuminator located on a side arm. The objective lens serves both as the condenser and the objective. A field diaphragm, and sometimes an aperture iris, are placed in the illuminating side arm together with the source collector at appropriate conjugate planes. The illuminating beam, commonly emitted by a xenon or mercury arc lamp, is filtered through a narrow band path interference filter and reflected down into the objective by a dichromatic beam splitter. The fluorescent imaging beam originating from the specimen passes straight through the dichromatic beam splitter and associated barrier filter and reaches the ocular. Each fluorescent cube contains the appropriate excitation interference filter, dichromatic beam splitter, and barrier filter so that they can be switched as a group, for example, to rapidly inspect specimens containing (or stained with) multiple fluorochrome.

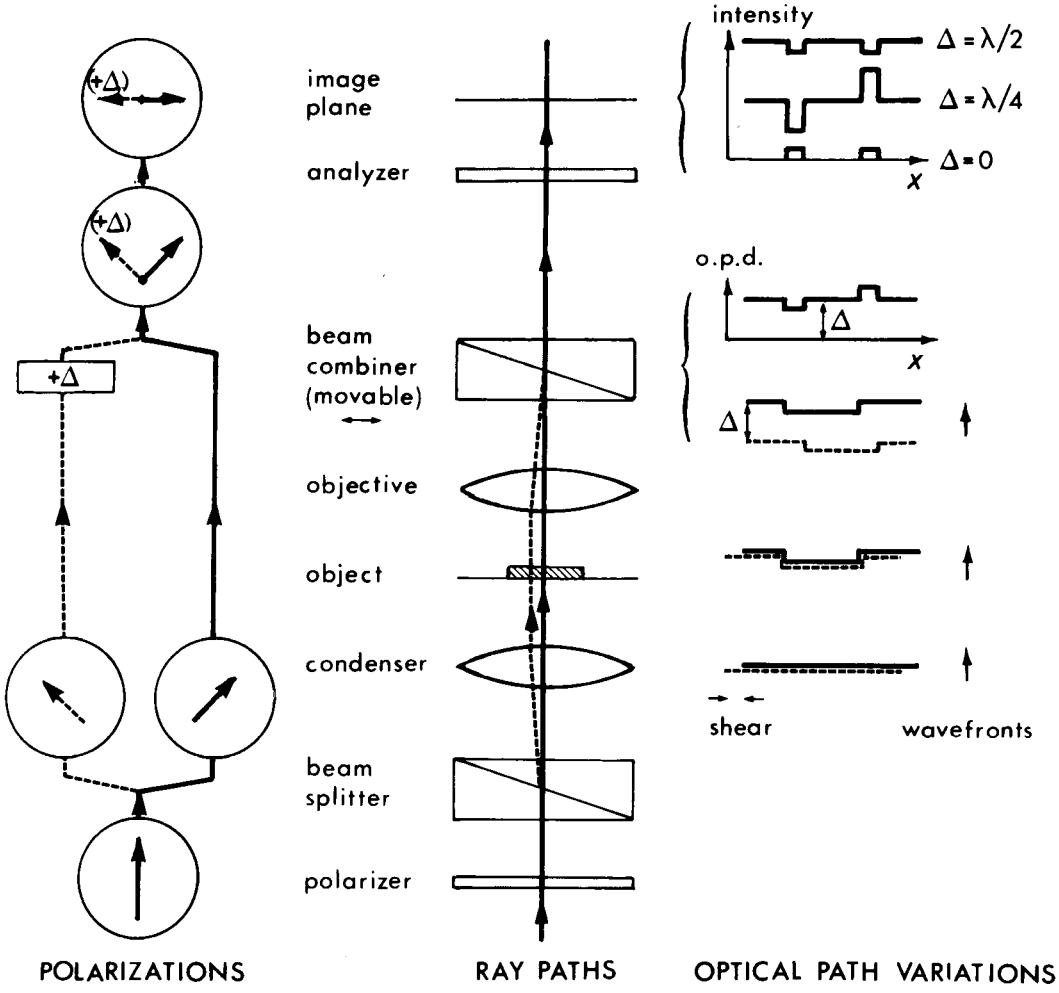

FIGURE 27 The optical system for differential interference contrast (DIC, see text).[65]

For fluorochrome requiring shorter-wave UV excitation, objective lenses must be designed for greater short-wavelength transmission and low autofluorescence. While aberrations for the shorter-UV exciting wavelengths are generally not as well-corrected as for the imaging wavelengths, it should be noted that such aberrations, or lack of parafocality, directly affect the resolution in the case of confocal fluorescence microscopes.

Also, it should be noted that, while little effort is commonly made to fill the objective aperture with the illuminating beam (presumably with the rationale that this should not affect image resolution because each fluorescent object is emitting incoherently relative to its close neighbor), one finds that in practice the fluorescent image is much improved by filling the aperture, for example, by use of an optical fiber light scrambler (see the section on "Transillumination" later in this chapter). (The reason for this improvement is still not fully understood—whether it is solely due to the increased level of illumination which, in turn, provides improved signal of the intrinsically low-light fluorescent image (but why

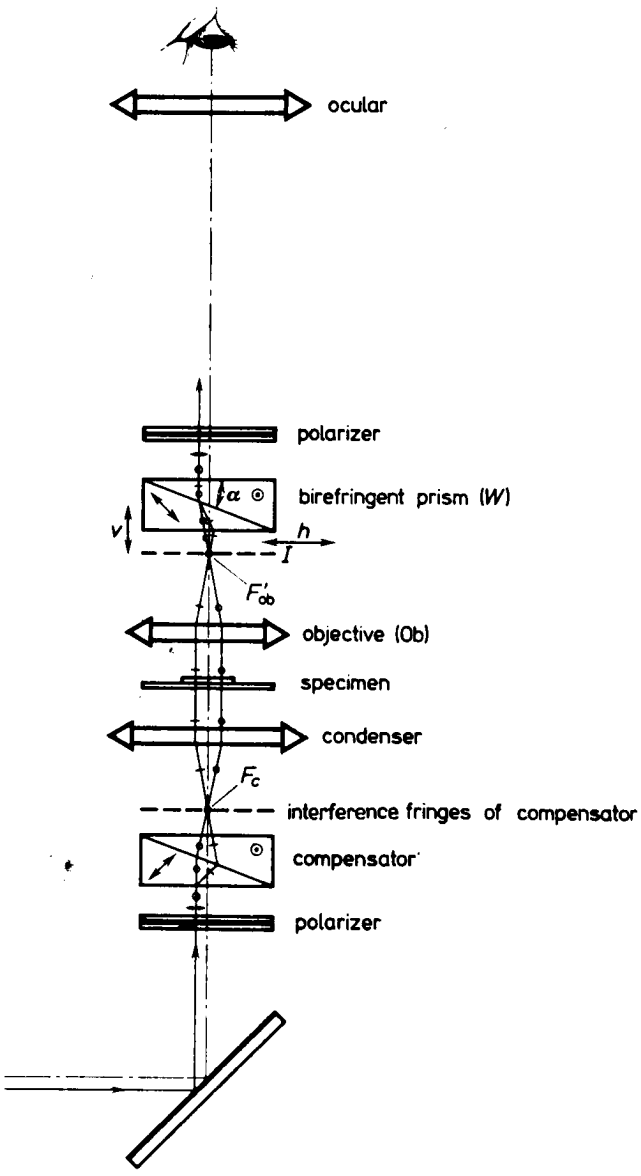

FIGURE 28 Standard Nomarski interference contrast with modified Wollaston prisms which are placed outside the focal planes of condenser and objective.[8]

should the scrambler improve the level of illumination to start with?) or whether NA_{cond} does affect resolution in fluorescence microscopy after all.)

While most fluorescence microscopes today use epi-illumination (since epi-illumination provides advantages such as avoiding loss of excitation by self-absorption by underlying fluorochrome layers, generating an image that more closely approximates an intuitive one

when reconstructed in three dimensions, etc.), improvements in interference filters open up new opportunities for fluorescence microscopy using transillumination. New interference filters are available with exceptionally high extinction ($>10^5$) and sharp cutoff of the excitation wavelengths, coupled with high transmission of the pass band. With transillumination, one can more reliably combine fluorescence with polarization-based microscopy or carry out polarized fluorescence measurements with greater accuracy, since one can avoid the use of dichromatic beam splitters which tend to be optically anisotropic.

Fluorescence microscopy particularly benefits from video imaging, especially with the use of low-noise, chilled CCDs as imaging detectors, digital computers to enhance and rapidly process the signal (such as in ratio imaging), and the new fluorescence-conjugated chemical probes that provide incredible sensitivity and selectivity (see also pp. 17.46–17.48).[9–11,34]

17.6 ILLUMINATION AND IMAGING MODES

Transillumination

The full impact of the illumination system on the final quality of the microscope image is often not appreciated by the microscope user or designer. Undoubtedly, part of this neglect arises from a lack of understanding of the roles played by these components, in particular the condenser, and the common practice of closing down the condenser iris diaphragm to adjust image contrast for comfortable viewing. Also, it may in part stem from Zernicke's consideration that the microscope resolution is independent of the condenser's correction (cited, e.g., in Ref. 35). Regardless of the conventional view, critical examination of the microscope image or point spread function reveals the importance of the alignment, focus, tilt, NA, and effective aperture function of the condenser. The effects are especially noticeable when contrast is enhanced, e.g., by video microscopy.

The theoretical influence of condenser NA on image resolution has been calculated by Hopkins and Barham,[36] who showed that maximum resolution could be obtained at $\mathrm{NA_{cond}} = 1.5 \times \mathrm{NA_{obj}}$ (Fig. 29). Such high $\mathrm{NA_{cond}}$ is usually not achievable for high-NA objective lenses, and, in addition, with most objectives, flare due to internal reflection would reduce image contrast to an extent possibly unsalvageable even with video contrast enhancement. For $\mathrm{NA_{cond}} \leq \mathrm{NA_{obj}}$, the minimum resolvable distance between two point objects is commonly given by the formula:

$$d = \frac{1.22\lambda}{\mathrm{NA_{obj}} + \mathrm{NA_{cond}}} \tag{11}$$

which expresses the importance of $\mathrm{NA_{cond}}$ on resolution. Again, reduction of $\mathrm{NA_{cond}}$, generally achieved by closing down the condenser iris diaphragm, tends to raise image contrast so that even experienced microscopists tend to use an $\mathrm{NA_{cond}} \approx (0.3 \cdots 0.5) \times \mathrm{NA_{obj}}$ to obtain a compromise between resolution and visibility. With video and other modes of electronic enhancement, the loss of contrast can be reversed so that improved lateral, and especially axial, resolution is achieved by using an $\mathrm{NA_{cond}}$ that equals, or nearly equals, the $\mathrm{NA_{obj}}$. With a larger $\mathrm{NA_{cond}}$, the S/N ratio is simultaneously improved by the increased photon flux that illuminates the specimen.

Under optimum circumstances, the light source and condenser should be focused for Köhler illumination (Fig. 5) to minimize flare and to improve the homogeneity of field illumination. Alternately, image brightness, especially in the middle of the field, can be maximized by *critical illumination* where the condenser is somewhat defocused from Köhler illumination to produce an image of the source rather than the field diaphragm

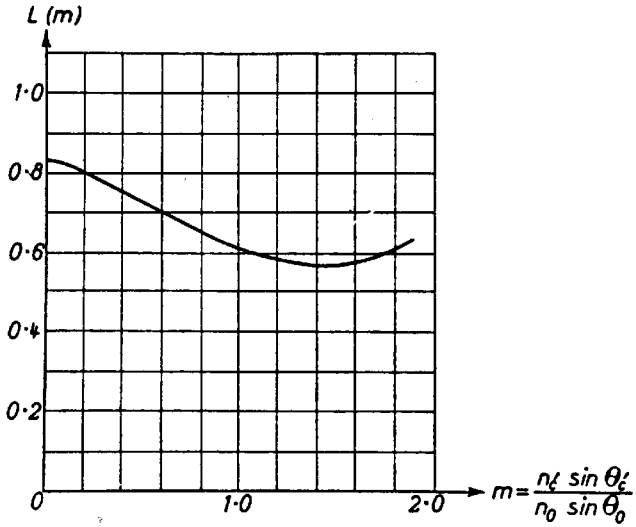

FIGURE 29 Effect of the condenser aperture on the resolution of two pinholes of equal brightness. m is the ratio of the numerical apertures of condenser to objective. L is the minimum resolved distance between the pinholes (Rayleigh criterion) in units of the wavelength divided by the objective aperture.[35]

superimposed on the specimen. Either mode of illumination can yield resolution approximately as given by Eq. (11).

The aperture function of the microscope can become nonuniform, or limited, for a number of reasons, These include misalignment between the objective and condenser lenses; misalignment of the condenser iris (relative to the condenser lens elements); misalignment of the illuminator and condenser axes; tilted objective or condenser lenses or lens elements; nonuniform illumination of the condenser aperture; limited source size; nonuniform intensity distribution in the source; and improper choice, or focusing, of the condenser or source collector. Whether intentional or accidental, these conditions can reduce the effective NA_{cond} and/or induce oblique illumination, thus sacrificing resolution and image quality. An improvement, using a single optical fiber light scrambler, that allows the filling of the full condenser aperture with uniform illumination and little loss of field brightness (especially when using concentrated arc lamps) was introduced by Ellis[37] (also see Figs. III-21, III-22 in Ref. 6).

Epi-illumination

In the epi-illumination mode, a beam splitter, part-aperture-filling mirror, or wavelength-discriminating dichromatic (unfortunately often called dichroic) mirror, placed behind the objective lens diverts the illuminating beam (originating from a light source placed in the side arm of the microscope) into the objective lens which also acts as the condenser (Fig. 30). Alternatively, a second set of lenses and a beam-diverting mirror (both of whose centers are bored out and are arranged coaxially around the objective lens) can provide a larger-NA illuminating beam, much as in dark field illumination in the transillumination mode.

This latter approach limits the maximum NA of the objective lens to around 1.25, but has the advantage that the illuminating beam traverses a path completely isolated from

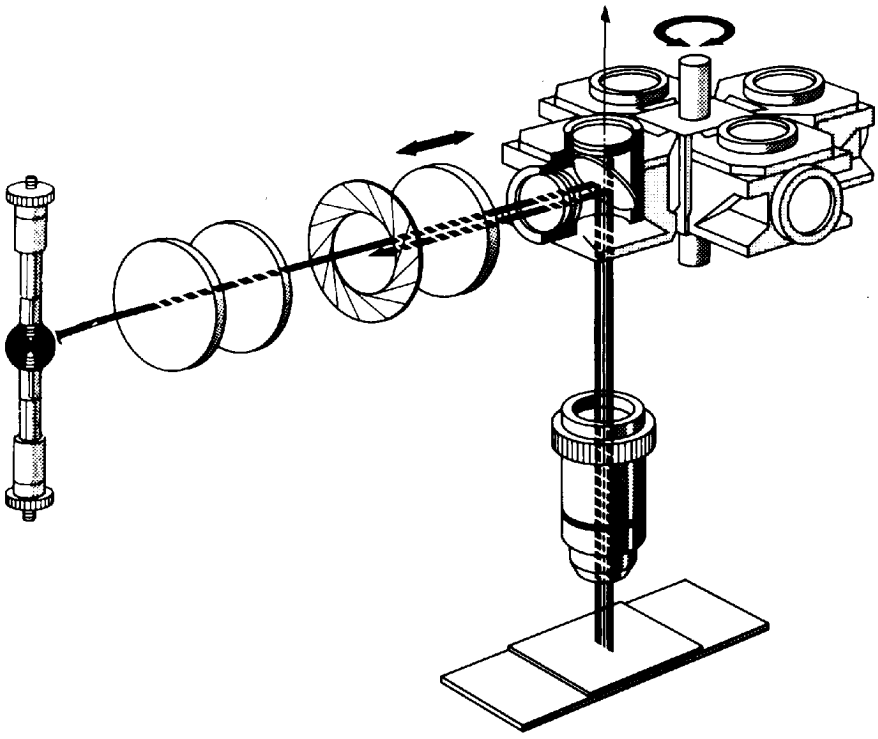

FIGURE 30 Schematic of epi-illuminating light path. The rotatable set of filter cubes with excitation filters, dichromatic mirrors, and barrier filters matched to specific fluorochromes are used in epifluorescence microscopy.[66]

the image-forming beam. When the two beams do pass through the same objective lens, as is the case with most epi-illuminating systems, the lens elements must be carefully designed (by appropriate choice of curvature and use of highly efficient antireflection coating) to reduce hot spots and flare introduced by (multiple) reflection at the lens surfaces. Modern microscope objectives for metallurgical and industrial epi-illuminating systems in particular are designed to meet these qualities. In addition, circular polarizers (linear polarizers plus $\lambda/4$ wave plates) and appropriate stops are used to further exclude light reflected from the surfaces of lens elements, cover glass, etc. For epi-illumination fluorescence microscopy, dichromatic beam splitters and barrier filters can reduce background contamination that arises from the exciting beam to less than one part in 10^4.

Orthoscopic vs. Conoscopic Imaging

The common mode of observation through a microscope is by orthoscopic observation of the focused image. For certain specific applications, particularly with polarizing microscopes, examination of the aperture plane, or conoscopic observation, sheds valuable complementary information.

Conoscopic observation can be made either by replacing the regular ocular with a telescope that brings the aperture plane into focus or by inserting a Bertrand lens (that serves as a telescope objective) in front of a regular ocular. Conversely, one can observe the aperture plane simply by removing the ocular and looking down the microscope body

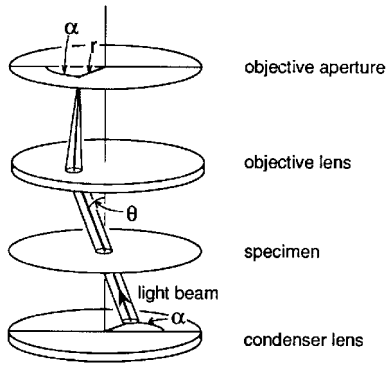

FIGURE 31 Parallel rays with inclination θ and azimuth orientation α, traversing the specimen plane, and focused by the objective lens at a point with radius r and same azimuth angle α in the aperture plane.

tube (in the absence of a Bertrand lens) or by examining the Ramsden disk above the ocular with a magnifier.

The polar coordinates of each point in the aperture plane, i.e., the radius r and azimuth angle α, are related to the rays traversing the specimen by: $r = \sin\theta$ and α = (azimuth orientation of the ray projected onto the aperture plane) (Fig. 31). Thus, conoscopic observation provides a plane projection of all of the rays traversing the specimen in three-dimensional space. For specimens, such as single crystal flakes or polished mineral sections in which a single crystal is illuminated (optically isolated) by closing down the field diaphragm, the conoscopic image reveals whether the crystal is uniaxial or biaxial, its optic axis angle and directions, as well as sign and strength of birefringence and other anisotropic or optically active properties of the crystal.[24]

Conoscopic observation also reveals several attributes of the condenser aperture plane and its conjugate planes (e.g., in Köhler illumination, the plane of the condenser iris diaphragm and the illuminating source). Thus, conoscopy can be used for checking the size, homogeneity, and alignment of the illuminating light source as well as the size and alignment of the condenser iris diaphragm and phase contrast annulus (located at the front focal plane of the condenser) relative to the objective exit pupil or the phase ring (located at the back focal plane of the objective). It also reveals the state of extinction in polarized light and interference contrast microscopy and provides a visual estimate of the aperture transfer function for the particular optical components and settings that are used.

The aperture plane of the microscope is also the Fourier plane of the image, so that diffraction introduced by periodic texture in the specimen can be visualized in the aperture plane by conoscopic observation. Depending on the NA of the objective and the spatial period in the specimen, the pattern of diffraction up to many higher orders can be visualized when the condenser iris is closed down and laterally displaced to illuminate the specimen with a narrow, oblique, coherent (monochromatic) beam, and the zero-order intensity is suppressed (e.g., by the use of appropriate polarizers and compensator).

Confocal Microscopy

In confocal microscopy, the specimen is scanned point by point either by displacing the specimen (stage scanning) or by scanning a minute illuminating spot (beam scanning), generally in a TV-raster fashion. In either case, the scanning spot is an Airy disk formed by a high-NA objective lens. An exit pinhole is placed conjugate to the spot being scanned so

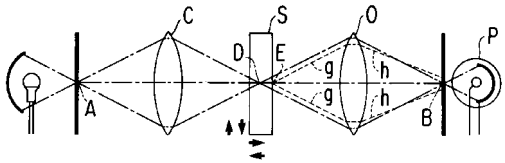

FIGURE 32 Optical path in simple confocal microscope. The condenser lens *C* forms an image of the first pinhole *A* onto a confocal spot *D* in the specimen *S.* The objective lens *O* forms an image of *D* into the second (exit) pinhole *B* which is confocal with *D* and *A.* Another point, such as *E* in the specimen, would not be focused at *A* or *B,* so that the illumination would be less and, in addition, most of the light *g-h* scattered from *E* would not pass the exit pinhole. The light reaching the phototube *P* from *E* is thus greatly attenuated compared to that from the confocal point *D.* In addition, the exit pinhole could be made small enough to exclude the diffraction rings in the image of *D*, so that the resolving power of the microscope is improved. The phototube provides a signal of the light passing through points D_1, D_2, D_3, etc. (*not shown*), as the specimen is scanned. D_1, D_2, D_3, etc. can lie in a plane normal to the optical axis of the microscope (as in conventional microscopy), or parallel to it, or at any angle defined by the scanning pattern, so that optical sections can be made at angles tilted from the conventional image plane. Since, in the stage-scanning system, *D* is a small spot that lies on the axis of the microscope, lenses *C* and *O* can be considerably simpler than conventional microscope lenses.[38,67]

that only the light originating from the scanned spot is transmitted through the exit pinhole. Thus, light originating from other regions of the specimen or optical system are prevented from reaching the photo detector (Fig. 32).

This optical arrangement reduces blurring of the image from out-of-focus light scattering, fluorescence, etc., and yields exceptionally clear, thin optical sections. The optical sections can then be processed and assembled electronically to yield three-dimensional displays or tilted plane projections. Alternatively, the specimen itself can be scanned through a tilted plane (e.g., by implementing a series of x scans with y, z incremented) to yield a section viewed from any desired orientation, including that normal to the microscope axis.

In addition to yielding optical sections with exceptional image (S/N) quality, confocal microscopes of the stage-scanning type can be used to vastly expand the field of view. Here the image area is not limited by the field of view of the optics but only by the range of movement of the specimen and ability of the photo detector and processor to handle the vast information generated at high speed. Furthermore, the objective lens needs only to be corrected for a narrow field of view on axis.[5,38] Laser disk recorders are a form of application that takes advantage of these attributes.

Beam-scanning confocal microscopes can be classified into two types. In the *disk-scanning* type, the source and exit pinholes, arranged helically on a modified Nipkow disk, concurrently scan (1) the field plane that is located in front of the collector lens of the light source and (2) the image plane of the objective lens. By using epi-illumination, these two planes lie at the same distance, both above the objective lens. Thus, a single spinning disk (with symmetrically placed pinholes that alternatively serve as entrance and exit pinholes in the Petráň type, or used with a beam splitter so that each pinhole serves both as

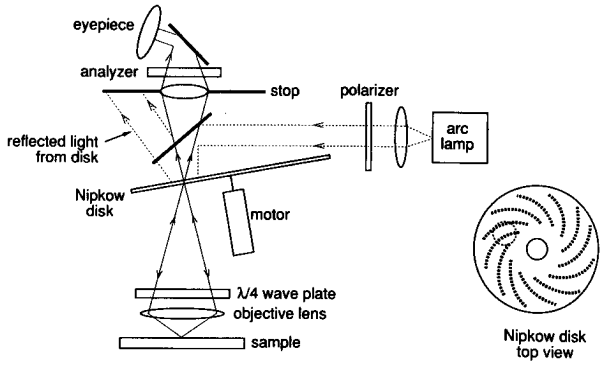

FIGURE 33 Kino-type real-time confocal microscope (see text).[40]

entrance and exit pinholes in the Kino type) can be made to provide synchronously scanning entrance and exit pinholes (Fig. 33).[39,40] The *disk-scanning* type confocal microscope suffers from light loss due to the small areas occupied by the pinholes (even though several pinholes are made to scan the field simultaneously) but has the advantage of permitting direct visual viewing of the confocal image.

In a confocal microscope, the exit pinhole can be made smaller than the diameter of the Airy diffraction image formed by the objective lens so that the Airy disk is trimmed down to regions near its central peak. With this optical arrangement, the unit diffraction pattern that makes up the image turns out to be the square of the Airy pattern given in Eq. (2). Thus, the radius at half maximum of the central bright area (Airy disk) is reduced by a factor of 1.36. (The radial position of the first minimum in both patterns is still equal to r_{Airy}.) The shape of the unit diffraction pattern is thus sharpened so that, compared to nonconfocal imaging, two points which radiate incoherently (as in fluorescence microscopy) can be expected to approach each other by up to a factor of $\sqrt{2}$ closer to each other before their diffraction patterns encounter the Rayleigh limit. Figure 18 compares the contrast transfer characteristics of a confocal microscope in the coherent imaging mode with the same lenses used in the nonconfocal, incoherent imaging mode.

In the laser-scanning epi-illuminating confocal microscope (which was developed into a practical instrument in the late 1980s and immediately adopted with great enthusiasm), a source pinhole is commonly omitted since the focused beam of the single-mode (TEM_{00}) laser itself produces a pointlike source. This source is expanded by relay lenses (or mirrors) and the ocular to fully cover the back aperture of a very well-corrected, flat-field objective lens and then focused onto the specimen where it forms a minute Airy disk defined by the NA of the objective and wavelength of the laser source. The Airy disk formed by the objective is scanned in the x, y image plane by two galvanometer mirrors placed at the eyepoint of the ocular (or its conjugate plane in order to insure that the direction of the rays alone is deviated at the aperture plane and that the objective aperture remains fully illuminated throughout the scanning). Viewed from the specimen towards the source, the two mirrors swing the source image (in sawtooth waves rapidly along the x direction and slowly along the y direction) so that the specimen is scanned along these orthogonal axes in a raster pattern by the Airy spot formed by the objective lens.

The scanned spot is imaged by the same set of lenses, and the image-forming beam is deviated by the same two sets of swinging mirrors, in reverse order, so that the image of the scanned spot becomes stationary at its image plane. The paths of the illuminating beam and the return imaging beam are shared until the two paths are separated by a (dichromatic) beam splitter into: (1) the path from the laser, and (2) the path to the exit

pinhole. The location of the exit pinhole is adjusted to lie in the conjugate image plane coaxially with the source point, therefore, confocal with the source point and the scanning spot. The confocally adjusted exit pinhole intercepts the final Airy disk formed by the objective lens and trims away the surrounding rings as well as the outer foot of the disk. Depending on the amount of light available (or tolerable by the specimen) and the permissible scan duration for forming the image, a compromise is often needed between reduction of the exit pinhole diameter (that improves image resolution and optical sectioning capability) and expansion of the pinhole diameter to allow more light to reach the photodetector. When the need to acquire confocal images at high rate is frustrated by the limited amount of light reaching the photodetector, the exit pinhole can be replaced by a slit, with surprisingly little deterioration of optical sectioning capability.

Rather than using confocal optics to eliminate image blurring from out-of-focus planes, one can achieve the same end by computational deconvolution of a stack of serial optical sections obtained by video microscopy.[17,41] While computationally intensive and time consuming, this image restoration method allows one to isolate clean optical sections from a stack of images that can be acquired at a much higher speed than with laser-scanning confocal microscopy and in modes of contrast generation not accessible to confocal imaging.

Alternatively, thin optical sections can be obtained directly with digital enhanced video microscopy using high-NA condenser and objective lenses. Requiring little processing, this approach is especially convenient when many stacks of optical sections have to be acquired at high rates in succession, e.g., in order to record rapid, three-dimensional changes in microscopic domains over time.

Proximity-scanning Microscopy

A microscope's limit of resolution [Eq. (1)] can be exceeded by narrowing the field of illumination. In confocal microscopy, the resolution is expected to be improved by up to a factor of $\sqrt{2}$ by illuminating the field point by point with an Airy diffraction spot and by using a small confocal exit pinhole. Even in the absence of confocal optics, Harris[42] has argued that the diffraction pattern in the Fourier plane can be extrapolated beyond the spatial frequency that is cut off by the NA of the objective lens—in other words, that the limit of resolution can be exceeded by computational extrapolation of the diffraction orders as long as the specimen is illuminated in a narrowly limited field.

The field of illumination can be reduced beyond that defined by diffraction by placing the minute exit aperture of a tapered light guide or a minute pinhole closely adjacent to the specimen. By scanning such an aperture relative to the specimen, one obtains a proximity-scanned image whose resolution is no longer limited by the diffraction orders captured by the objective lens. Instead, only the size of the scanning pinhole and its proximity to the specimen limit the resolution.[43]

For non-optical microscopes, e.g., in scanning tunneling, force, and other proximity-scanning microscopes, resolution down to atomic dimensions can be obtained on images that reflect topological, electronic, ionic, and mechanical properties of the specimen surface.[44] In these types of proximity-scanning microscopes, a fine-tipped probe, mounted on a piezoelectric transducer that provides finely controlled x, y, and z displacements of the probe, interacts with specific properties of the specimen surface (alternatively, the probe may be fixed and the sample mounted to the transducer). The resulting interaction signal is detected and fed back to the z-axis transducer, which generally induces the probe tip to rise and fall with the surface contour (that reflects the particular electrical or mechanical property of the surface) as the probe is scanned in a raster fashion along the x and y directions over an area several tens of Ångstroms to several tens of micrometers wide. A highly magnified contour image of the atomic or molecular lattices is generated on a monitor that displays the z signal as a function of the x, y position.

Aperture Scanning

In the aperture-scanning microscope devised by Ellis[45] for phase contrast microscopy, the tip of a flexible signal optical fiber, illuminated by an Hg arc, makes rapid circular sweeps at the periphery of the condenser aperture. This circular, scanning illumination spot replaces the conventional phase annulus in the condenser aperture plane. A quarter-wave plate and absorber, both covering only a small area conjugate to the illuminating spot, spins in synchrony with the fiber at the objective back aperture (or its projected conjugate). Thus, the specimen is illuminated by a narrow, coherent beam that enters the specimen obliquely at high NA, with the azimuth orientation of the beam swinging around and around to generate a full cone of illumination within the integration time of the detector. With this aperture-scanning approach, the specimen is illuminated by a large-NA cone of light which is temporally incoherent, with the phase disk covering only a small fraction of the area normally occupied by the phase ring in conventional phase contrast systems. The small size of the phase disk, while appropriately reducing the amplitude and introducing the requisite 1/4 wave phase retardation to the rays not scattered by the specimen, allows the transmission of a much larger fraction of the scattered rays that carry the high spatial frequency information. The aperture-scanning phase contrast microscope thus provides a very thin optical section. The image is also virtually free of the phase halo that obscures image detail adjacent to refractile boundaries in conventional phase contrast microscopy.

Extending this concept, modulation of the transfer functions of the condenser and objective apertures with electro-optical devices should open up intriguing new opportunities. Such modulation eliminates the need for mechanical scanning devices, the spatial distribution of the modulation function can be altered at will, and the amplitude and phase of light passing each point in the aperture can be adjusted rapidly, even coupled dynamically to the image signal through a feedback loop to generate dynamic spatial filters that enhance or select desired features in the image.

Video Enhancement and Digital Image Processing

Video and related forms of electronic imaging offer a number of advantages that vastly extend the utility of the light microscope. The electronic signal generated by the video camera can be readily amplified and biased to boost contrast in desired gray-value ranges of the image while suppressing unwanted background signal noise and light due to flare, inadequate extinction, etc. (Fig. 34). Through such analog processing, one gains the opportunity to use objective lenses at higher condenser NA, and in contrast modes that previously could not generate an image with high enough contrast for direct observation. Thus, in DIC, polarized light, and other modes of microscopy, one can now use

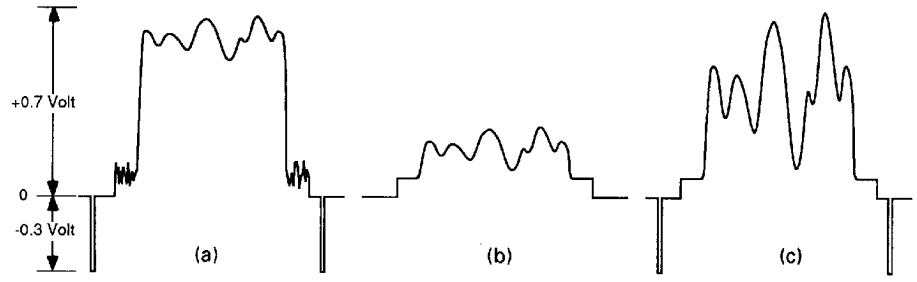

FIGURE 34 Analog contrast enhancement of video signal: (*a*) original signal; (*b*) sync pulses removed and signal level adjusted to suppress background noise; (*c*) signal amplified and sync pulses added back.

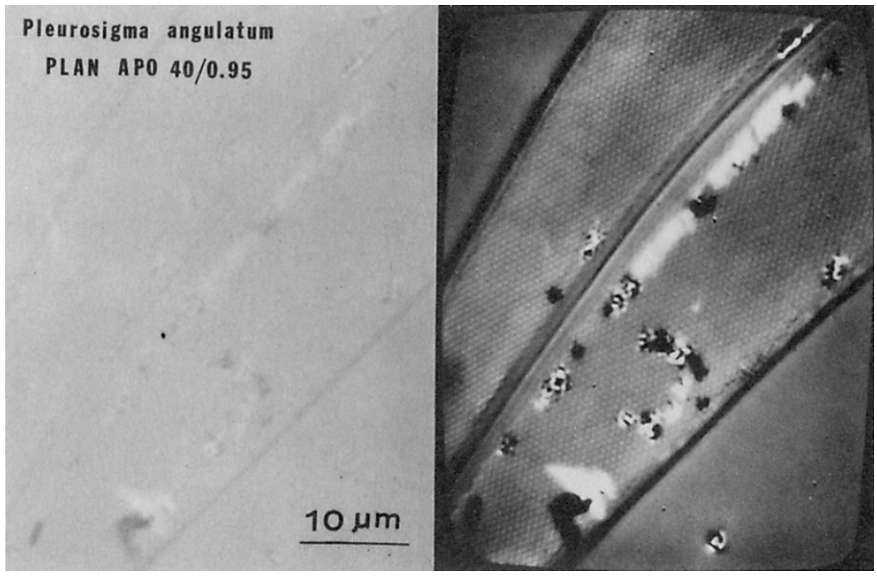

FIGURE 35 Diatom frustule viewed between crossed polarizers and a $\lambda/10$ compensator without (*left*) and with (*right*) analog video enhancement.[68]

better-corrected lenses, such as the 1.4 NA Plan Apo objective illuminated with matched-NA condenser, to generate images with greater resolution coupled with vastly improved contrast for objects that previously could barely be detected (Fig. 35).

Compared to visual observation or photography, which are based on logarithmic responses of photochemical detectors, an ideal video signal responds linearly to image intensity. Thus, in addition to analog enhancement, the video signal can be digitized in a straightforward fashion and processed with a digital computer. Today, the video signal can be digitized (e.g., to 640×480 pixels at 256 gray levels) and processed at video frame rate (30 frames/s) with a fairly simple personal computer to which is added an imaging board that contains digitizers, look-up tables, frame stores, video bus, logic units, and flexible operational and routing alternatives. These functions are controlled by software residing in the host computer. With such a digital image processor, one can carry out a large variety of operations, much of them on line, at video rate, including image capture, storage, grayscale stretching, binarizing; interimage manipulations such as averaging, subtraction, superposition, ratio imaging, selection of minimum or maximum value pixels; interpixel manipulations such as spatial filtering, gradient differentiation, unsharp masking; and many forms of (automatic) quantitative analyses of image geometrics and intensities. With such digital image processors, image defects due to uneven microscope illumination or fixed pattern noise can simply be subtracted away, noise in low-light-level images can be suppressed by frame averaging or spatial filtering, and contrast and desired spatial frequencies can be boosted or suppressed, etc. (Fig. 36).

Not only does analog and digital image processing permit the full use of the light microscope to deliver the theoretical maximum resolution in contrast modes and on specimens that hitherto escaped detection, but the clean, high contrast image provides opportunities for direct observation of the dynamic behavior of individual, unresolvable molecular filaments and membranes. The image of these nanometer-thick filaments (expanded to their Airy disk diameter) clearly depicts their mobility, polymerization-depolymerization, interaction with organelles in living cells, etc. Thus, new insights are

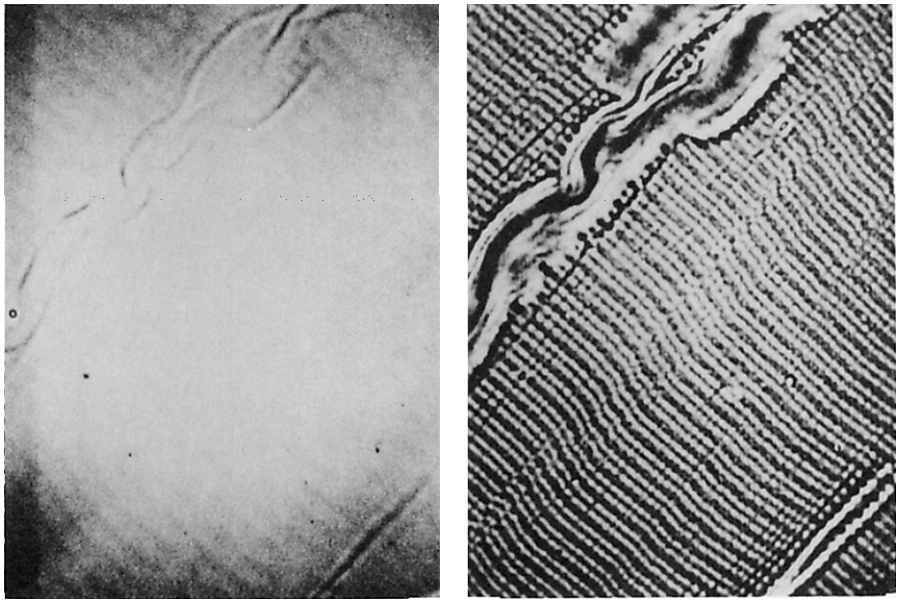

FIGURE 36 Muscle thin section in matched index medium (totally invisible without video enhancement). With analog video enhancement (*left*); with analog and digital enhancement (*right*). (*Reproduced from American Laboratory, April 1989.*)

gained by observing the behavior of individual macromolecular assemblies that were not anticipated from conventional chemical analyses that relied on statistical behavior of large numbers of sample molecules.

In addition to extending the applicable range of image detection and maximizing the attainable resolution in the x–y plane, the digitally processed, high-NA video images provide clearer and thinner optical sections. The effects of video enhancement on z-axis resolution and optical sectioning is all the more striking since they rise as the square of operative NA as contrasted to the linear rise of lateral resolution with NA.

Ratio Imaging

The concentration of minute quantities of specific ions and chemicals can be measured accurately in living cells and other irregularly shaped objects by fluorescence ratio imaging. For example the pH, and micromolar to nanomolar concentrations of calcium ions, can be measured in pico- to femtoliter volumes in active nerve and kidney cells preloaded with fluorescent reporter dyes such as SNARF and Fura-2.[10,34] The concentrations, as well as the spreading waves of the pH or calcium ion within the cell, can be followed second-by-second with a digital processor coupled to a fluorescence microscope equipped with low-light-level video camera and illuminated alternatively with, for example 340- and 380-nm excitation wavelengths. The reporter dye is formulated so as to emit fluorescence as a sensitive function of the ion concentration at one of the two exciting wavelengths, while at the other exciting wavelength the emission does not vary (isosbestic point) or is an inverse function of the ion concentration. Thus, for each pixel, the ratio of fluorescence intensities emitted by the reporter dye excited at the two wavelengths provides the concentration of the ionic species independent of sample thickness and local dye concentration.

Three-dimensional Imaging

For low-power observations, the three-dimensional features of a specimen can be viewed directly under a dissecting microscope equipped with pairs of tilted objectives, erecting prisms, and oculars (Greenough type), or through a single larger objective lens whose aperture is divided to provide the left- and right-eye images with appropriate stereoscopic parallax. With high-NA objectives, these approaches are not very effective owing to the shallow depth of field.

With the new capability to obtain serial optical sections through the highest-NA objectives using confocal or video-enhanced microscopy, and to rapidly store, retrieve, and manipulate the stored images in a digital computer, one can now generate stereoscopic and other three-dimensional views representing a substantial depth of the specimen at the highest resolution of the light microscope.[46] The stack of ultrathin optical sections can be used directly as acquired through the high-NA objectives or after digital deconvolution to further improve the quality of each optical section by reducing undesired contributions from out-of-focus fluorescence, light scattering, etc.[17,41]

17.7 OPTICAL MANIPULATION OF SPECIMEN WITH THE LIGHT MICROSCOPE

In confocal microscopy, light initially travels ''in a reverse path'' through an objective lens to form a diffraction-limited image of the source pinhole into the specimen plane. In a similar vein, the light microscope and microscope objectives are increasingly used to project reduced high-intensity images of source patterns into the object plane in order to manipulate minute regions of the specimen optically. Photolithography and laser disk recorders are examples of important industrial applications which have prompted the design of specially modified objective lenses for such purposes.

Microbeam Irradiation, Caged Compounds

Many applications are also found in the biomedical field, some using UV-transmitting, moderately high NA objectives that are parafocalized for visible light and UV down to approximately 250 nm (Zeiss Ultrafluar and catadioptric objectives from Cooke-A.E.I., also quartz monochromats from Leitz). In its extreme form, a concentrated image of a circular- or slit-shaped UV or laser source of selected wavelengths is imaged onto a biological specimen to locally ablate a small targeted organelle; for example, a part of a chromosome, the microtubules attached thereto, or tiny segments of cross-striated muscle, are irradiated with the microbeam in order to sever their mechanical connections and, for example, to analyze force transduction mechanisms.[47,48] In other cases, oriented chromophores can be selectively altered at the submolecular level, for example, by polarized UV microbeam irradiation. The stacking arrangement of the DNA nucleotide bases (which exhibit a strong UV dichroism, as well as birefringence in visible light) can be selectively altered and disclose the coiling arrangement of DNA molecules within each diffraction-limited spot in the nucleus of living sperm.[49] Brief microirradiation of slit- or grid-shaped patterns of UV are used to bleach fluorescent dyes incorporated into membranes of living cells. The time course of recovery of fluorescence into the bleached zone measures the rate of diffusion of the fluorescently tagged molecules in the membrane and reveals unexpected mobility patterns of cell membrane components.[50,51]

Also, selected target molecules within minute regions in living cells can be modified, tagged, or activated by focused beams of light. The target molecules can be naturally photosensitive species such as chlorophyll (which produces oxygen where illuminated with the appropriate visible wavelengths), rhodopsin (which isomerizes and triggers the

release of calcium ions and action potentials in retinal cells), or artificially introduced photosensitive reagents such as the drug colchicine (whose antimitotic activity is abolished locally with 366-nm irradiation).

Of the photosensitive compounds, the *caged compounds* promise a far-reaching potential. These are compounds that are synthesized so as to "cage" and hide the active chemical group until a photosensitive part of the compound is altered (e.g., by long-wavelength UV irradiation) and unmasks the hidden active group. Thus, by preloading with the appropriate caged compound and irradiating the cell selectively in the region of interest, one can test the role of the uncaged compound. For example, the role of ATP can be tested using caged ATP and ATP analogs; response to subtle increase in calcium ions can be seen using caged calcium or caged calcium chelators.[52,53] Likewise, caged fluorescent dyes are irradiated to locally label and follow the transport of subunits within macromolecular filaments in a dividing cell.[54]

Optical Tweezers

Intense laser beams concentrated into a diffraction spot can generate a photon-driven force great enough to capture and suspend small particles whose refractive index differs from its surrounding.[55] Applied to microscopy, a single swimming bacterium or micrometer-sized organelles in live cells can be trapped and moved about at will at the focus of a near-infrared laser beam focused by an objective lens of high NA. While the energy density concentrated at the laser focus is very high, the temperature of the trapped object remains within a degree or so of its environment; biological targets typically exhibit low absorbance at near-infrared wavelengths and thermal diffusion through water from such minute bodies turns out to be highly effective. Thus, the bacterium continues to multiply while still trapped in the focused spot, and it swims away freely when the laser beam is interrupted.

The ability to use "optical tweezers," not only to capture and move about minute objects but to be able to instantly release the object, provides the microscopist with a unique form of noninvasive, quick-release micromanipulator.[56]

17.8 MECHANICAL STANDARDS

Some mechanical dimensions for the light microscope have gradually become standardized internationally (Fig. 37, Table 6). While the standards permit more ready interchange of

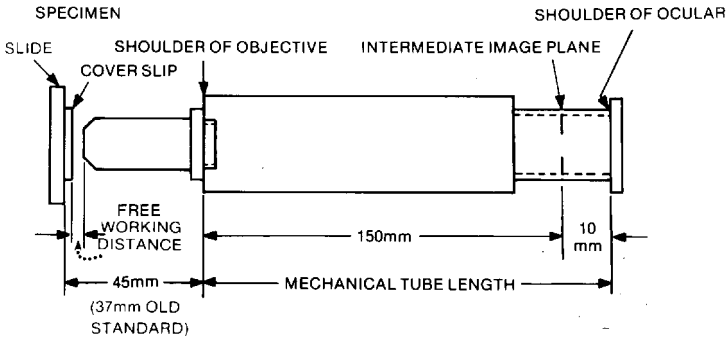

FIGURE 37 Dimensions for standard microscopes with finite focus objectives. See text section on "Tube Lengths and Tube Lenses for which Microscope Objectives Are Corrected" for further detail.[6]

TABLE 6 Royal Microscopical Society Standardized Objective Screw Thread Dimensions (in mm)

Thread		Ext. diam.	Pitch diam.	Core diam.	Calc. play male/female	Allowance	Tolerance
Female	Max	20.396	19.944	19.492		+0.076	
	Min	20.320	19.868	19.416	Min. 0.046	0	0.076
Male	Max	20.274	19.822	19.370	Max. 0.198	−0.046	
	Min	20.198	19.746	19.294		−0.122	0.076

Based on data given in the specification by the RMS [*J. R. Microsc. Soc.* **56:**377–380 (1936)] and now standardized in ISO Standard 8038 (1985) and in BS 7012, pt. 4.

Standard for ocular tube diameter: 23.2 mm or 30.0 mm.

objective lenses, oculars, etc., of different makes, in order to achieve optimum correction one still needs to be alert to the design constraint assumed by each manufacturer (finite or infinity focus, tube length, type and thickness of coverslip and immersion medium, aberrations corrected in objective alone or in combination with tube lens or with ocular, field size, and wavelength for correction, etc.: see section on''Microscope Lenses, Aberations'' in this chapter). The safest approach is to use the objectives and oculars on the microscope body supplied, but for those well-versed in the art, standardized dimensions do allow for greater flexibility of choice and innovative application.

17.9 ACKNOWLEDGMENTS

The authors thank Yoshiyuki Shimizu and Hiroohi Takenaka from Nikon K. K. Japan, for providing a preprint and original figures of their most useful article on microscope lens design. The authors are also grateful to Ernst Keller of Carl Zeiss, Inc., Jan Hinsch of Leica, Inc., Mortimer Abramovitz of Olympus, Inc., and Lee Shuett and Mel Brenner of Nikon, Inc., for providing detailed data on microscope lenses. We are especially grateful to Gordon W. Ellis of the University of Pennsylvania and Katsuji Rikukawa of Nikon K. K., Yokohama, for extensive discussions regarding several contents of this article. The preparation of this article was supported in part by the National Institutes of Health grant R-37 GM31617 and National Science Foundation grant DCB-8908169 awarded to S. I. and National Institutes of Health grant R01 GM49210 awarded to R. O.

17.10 REFERENCES

1. L. C. Martin, *The Theory of the Microscope.* Blackie, London, 1966.
2. F. Zernicke, ''Phase Contrast, A New Method for the Microscopic Observation of Transparent Objects, *Physica* **9:**686–693 (1942).
3. D. Gabor, ''Microscopy by Reconstructed Wavefronts, *Proc. Roy. Soc. London* A **197:**454–487 (1949).
4. M. Françon, *Progress in Microscopy,* Row, Peterson, Evanston, Ill., 1961.
5. T. Wilson and C. Sheppard, *Theory and Practice of Scanning Optical Microscopy,* Academic Press, London, 1984.
6. S. Inoué, *Video Microscopy,* Plenum Press, New York, 1986.
7. M. Pluta, *Advanced Light Microscopy Vol I*: *Principles and Basic Properties,* Elsevier Science Publishing Co., Amsterdam, 1988.
8. M. Pluta, *Advanced Light Microscopy Vol. II*: *Specialized Methods,* Elsevier Science Publishing Co., Amsterdam, 1989.

9. Y.-L. Wang and D. L. Taylor, *Fluorescence Microscopy of Living Cells in Culture,* Part A, Academic Press, San Diego, 1989.
10. D. L. Taylor and Y.-L. Wang, *Flourescence Microscopy of Living Cells in Culture,* Part B, Academic Press, San Diego, 1989.
11. D. L. Taylor, M. Nederlof, F. Lanni, and A. S. Waggoner, ''The New Vision of Light Microscopy,'' *American Scientist* **80:**322–335 (1992).
12. L. W. Smith and H. Osterberg, ''Diffraction Images of Circular Self-radiant Disks,'' *J. Opt. Soc. Am.* **51:**412–414 (1961).
13. K. Svoboda, C. F. Schmidt, B. J. Schnapp, and S. M. Block ''Direct Observation of Kinesin Stepping by Optical Trapping Interferometry,'' *Nature* **365:**72 (1993).
14. S. Inoué, ''Imaging of Unresolved Objects, Superresolution and Precision of Distance Measurement with Video Microscopy, in D. L. Taylor and Y.-L. Wang (eds.), *Methods in Cell Biology,* Academic Press, New York, 1989, pp. 85–112.
15. H. E. Keller, ''Objective Lenses for Confocal Microscopy'' in J. B. Pawley (ed.), *Handbook of Biological Confocal Microscopy,* Plenum Publ. Corp., New York, 1990, pp. 77–86.
16. I. T. Young, ''Image Fidelity: Characterizing the Imaging Transfer Function,'' in D. L. Taylor and Y.-L. Wang (eds.), *Methods in Cell Biology,* Academic Press, New York, 1989, pp. 1–45.
17. D. A. Agard, Y. Hiraoka, P. Shaw, and J. W. Sedat, ''Fluorescence Microscopy in Three Dimensions,'' in D. L. Taylor and Y.-L. Wang (eds.), *Methods in Cell Biology,* Academic Press, San Diego, 1989, pp. 353–377.
18. E. M. Chamot and C. W. Mason, *Handbook of Chemical Microscopy,* 2d ed., John Wiley & Sons, New York, 1958.
19. B. Kachar, ''Asymmetric Illumination Contrast: A Method of Image Formation for Video Microscopy,'' *Science* **227:**766–768 (1985).
20. C. S. Izzard and L. R. Lochner, ''Formation of Cell-to-Substrate Contacts During Fibroblast Motility: An Interference-Reflection Study'' *J. Cell Sci.* **42:**81–116 (1980).
21. F. Zernicke, ''The Wave Theory of Microscopic Image Formation,'' in J. Strong (ed.), *Concepts of Classical Optics,* W. H. Freeman and Co., San Francisco, 1958, pp. 525–536.
22. A. H. Bennett, H. Osterberg, H. Jupnik, and O. W. Richards, *Phase Microscopy, Principles and Applications,* John Wiley & Sons, Inc., New York, 1951.
23. G. W. Ellis, ''Advances in Visualization of Mitosis in vivo,'' in E. Dirksen, D. Prescott, and C. F. Fox (eds.), *Cell Reproduction*: *In Honor of Daniel Mazia,* Academic Press, New York, 1978, pp. 465–476.
24. N. H. Hartshorne and A. Stuart, *Crystals and the Polarizing Microscope*: *A Handbook for Chemists and Others,* 3d ed., Arnold, London, 1960.
25. M. M. Swann and J. M. Mitchison, ''Refinements in Polarized Light Microscopy,'' *J. Exp. Biol.* **27:**226–237 (1950).
26. H. Kubota and S. Inoué, ''Diffraction Images in the Polarizing Microscope,'' *J. Opt. Soc. Am.* **49:**191–198 (1959).
27. S. Inoué and H. Kubota, ''Diffraction Anomaly in Polarizing Microscopes,'' *Nature* **182:**1725–1726 (1958).
28. C. J. Koester, ''Interference Microscopy: Theory and Techniques,'' in G. L. Clark (ed.), *The Encyclopedia of Microscopy,* Reinhold, New York, 1961, pp. 420–434.
29. R. Barer, ''Phase, Interference and Polarizing Microscopy,'' in R. C. Mellors (ed.), *Analytical Cytology,* 2d ed., McGraw-Hill, New York, 1959.
30. H. G. Davies, ''The Determination of Mass and Concentration by Microscope Interferometry,'' in J. F. Danielli (ed.), *General Cytochemical Methods,* Academic Press, New York, 1958, pp. 55–161.
31. F. H. Smith, ''Microscopic Interferometry,'' *Research* (London) **8:**385–395 (1955).
32. R. D. Allen, G. B. David, and G. Nomarski, ''The Zeiss-Nomarski Differential Interference Equipment for Transmitted Light Microscopy,'' *Z. wiss. Mikroskopie* **69:**193–221 (1969).

33. T. Tsuruta, ''Special Nomarski Prism,'' *Appl. Optics* **2:**98–99 (1990).
34. R. Y. Tsien, ''Fluorescent Probes of Cell Signaling,'' in W. M. Cowas, E. M. Shooter, C. F. Stevens, and R. F. Thompson (eds.), *Annual Review of Neuroscience,* Annual Reviews Inc., Palo Alto, 1989, pp. 227–253.
35. M. Born and E. Wolf, *Principles of Optics,* 6th ed., Pergamon Press, Elmsford, N.Y., 1980.
36. H. H. Hopkins and P. M. Barham, ''The Influence of the Condenser on Microscopic Resolution,'' *Proc. Phys. Soc. London* **63B:**737–744 (1950).
37. G. W. Ellis, ''Microscope Illuminator with Fiber Optic Source Integrator,'' *J. Cell Biol.* **101:**83a (1985).
38. M. Minsky, Microscopy Apparatus, U.S. Patent #3013467, 1957.
39. M. Petráň, M. Hadravsky, D. Egger, and R. Galambos, ''Tandem-scanning Reflected-light Microscope,'' *J. Opt. Soc. Am.* **58:**661–664 (1968).
40. G. S. Kino, ''Intermediate Optics in Nipkow Disk Microscopes,'' in J. B. Pawley (ed.), *Handbook of Biological Confocal Microscopy,* Plenum Press, New York, 1990, pp. 105–111.
41. W. A. Carrington, K. E. Fogarty, L. Lifschitz, and F. S. Fay, ''Three Dimensional Imaging on Confocal and Wide-field Microscopes,'' in J. B. Pawley (ed.), *Handbook of Biological Confocal Microscopy,* Plenum Press, New York, 1990, pp. 151–161.
42. J. L. Harris, ''Diffraction and Resolving Power,'' *J. Opt. Soc. Am.* **54:**931–936 (1964).
43. E. Betzig, A. Lewis, A. Harootunian, M. Isaacson, and E. Kratschmer, ''Near-field Scanning Optical Microscopy (NSOM); Development and Biophysical Applications,'' *Biophys. J.* **49:**269–279 (1986).
44. H. K. Wickramasinghe, ''Scanned-probe microscopes,'' *Scientific American* **261:**98–105 (1989).
45. G. W. Ellis, ''Scanned Aperture Light Microscopy,'' in G. W. Bailey (ed.), *Proceedings of the 46th Annual Meeting of the Electron Microscopy Society of America,* San Francisco Press, San Francisco, pp. 48–49 (1988).
46. J. K. Stevens, L. R. Mills, and J. E. Trogadis (eds.), *Three Dimensional Confocal Microscopy,* Academic Press, San Diego, 1993.
47. R. E. Stephens, ''Analysis of Muscle Contraction by Ultraviolet Microbeam Disruption of Sarcomere Structure,'' *J. Cell Biol.* **25:**129–139 (1965).
48. M. W. Berns, *Biological Microirradiation, Classical and Laser Sources,* Prentice-Hall, Englewood Cliffs, N.J., 1974.
49. S. Inoué and H. Sato, ''Deoxyribonucleic Acid Arrangement in Living Sperm,'' in T. Hayashi and A. G. Szent-Gyorgyi (eds.), *Molecular Architecture in Cell Physiology,* Prentice Hall, Englewood Cliffs, N.J., 1966, pp. 209–248.
50. D. E. Koppel, D. Axelrod, J. Schlessinger, E. L. Elson, and W. W. Webb, ''Dynamics of Fluorescence Marker Concentration as a Probe of Mobility,'' *Biophys. J.* **16:**1315–1329 (1976).
51. H. G. Kapitza, G. McGregor, and K. A. Jacobson, ''Direct Measurement of Lateral Transport in Membranes by Using Time-Resolved Spatial Photometry,'' *Proc. Natl. Acad. Sci. USA* **82:**4122–4126 (1985).
52. J. H. Kaplan and G. C. Ellis-Davies, ''Photolabile Chelators for the Rapid Photorelease of Divalent Cations,'' *Proc. Natl. Acad. Sci. USA* **85:**6571–6575 (1988).
53. J. A. Dantzig, M. G. Hibberd, D. R. Trentham, and Y. E. Goldman, ''Cross-bridge Kinetics in the Presence of MgADP Investigated by Photolysis of Caged ATP in Rabbit Psoas Muscle Fibres,'' *J. Physiol.* **432:**639–680 (1991).
54. T. J. Mitchison and E. D. Salmon, ''Poleward Kinetochore Fiber Movement Occurs during both Metaphase and Anaphase-A in Newt Lung Cell Mitosis,'' *J. Cell Biol.* **119:**569–582 (1992).
55. J. M. Dziedzic, J. E. Bjorkholm, and S. Chu, ''Observation of a Single Beam Gradient Force Optical Trap for Dielectric Particles,'' *Optics Letters* **11:**288–290 (1986).
56. S. M. Block, ''Optical Tweezers: a New Tool for Biophysics,'' *Mod. Cell Biol.* **9:**375–402 (1990).
57. J. R. Benford, ''Microscope Objectives,'' in R. Kingslake (ed.), *Applied Optics and Optical Engineering,* Academic Press, New York, 1965, pp. 145–182.

58. S. Bradbury, P. J. Evennett, H. Haselmann, and H. Piller, *Dictionary of Light Microscopy,* Oxford University Press, Oxford, 1989.
59. E. Hecht, *Optics,* Addison-Wesley Publ. Co., Reading, Mass., 1987.
60. M. Cagnet, M. Françon, and J. C. Thrierr, *Atlas of Optical Phenomena,* Springer Verlag, Berlin, 1962.
61. Y. Shimizu and H. Takenaka, ''Microscope Objective Design'', in C. Sheppard and T. Mulvey (eds.), *Advances in Optical and Electron Microscopy,* vol. 14, Academic Press, San Diego, 1994, pp. 249–334.
62. R. Oldenbourg, H. Terada, R. Tiberio, and S. Inoué, ''Image Sharpness and Contrast Transfer in Coherent Confocal Microscopy,'' *J. Microsc.,* **172:**31–39 (1993).
63. R. Hoffman and L. Gross, ''Modulation Contrast Microscopy,'' *Appl. Optics* **14:**1169–1176 (1975).
64. S. Inoué and W. L. Hyde, ''Studies on Depolarization of Light at Microscope Lens Surfaces II. The Simultaneous Realization of High Resolution and High Sensitivity with the Polarizing Microscope,'' *J. Biophys. Biochem. Cytol.* **3:**831–838 (1957).
65. M. Spencer, *Fundamentals of Light Microscopy,* Cambridge University Press, London, 1982.
66. E. Becker, *Fluorescence Microscopy,* Ernst Leitz Wetzlar GmbH, Wetzlar, 1985.
67. S. Inoué, ''Foundations of Confocal Scanned Imaging in Light Microscopy,'' in J. B. Pawley (ed.), *Handbook of Biological Confocal Microscopy,* Plenum Publ. Corp., New York, 1990, pp. 1–14.
68. S. Inoué, ''Video Imaging Processing Greatly Enhances Contrast, Quality and Speed in Polarization-based Microscopy,'' *J. Cell Biol.* **89:**346–356 (1981).